STUDIES IN D.C. GLOW DISCHARGES IN HYDROGEN AND AIR WITH PARTICULAR REFERENCE TO EXTERNAL IRRADIATION BY VISIBLE LIGHT.

Being a thesis for the degree of

DOCTOR OF PHILOSOPHY.

Submitted by

ACHYUT P. THATTE,

Electronics Section, Department of Engineering,

UNIVERSITY OF EDINBURGH.

November, 1954.

TABLE OF CONTENTS.

GLOSSARY OF SYMBOLS USED.

A	Amperes.
A	Area.
A^+	Positive ion of gas A.
A^-	Negative ion of gas A.
A^*	Excited state of an atom or molecule of gas A.
C	Capacity.
$\bar{c}$	Velocity of agitation.
c/s	Cycles per second.
D	Diameter of the discharge tube.
d	diameter of the side-arm.
d	Diameter of the conductors of the parallel transmission line.
$\bar{d}$	Average distance which an electron moves in a field X.
$\bar{E}$	Average electron energy.
e	Charge on an electron.
H	Atom of hydrogen.
H_2	Molecule of hydrogen.
h	Plank's constant.
h	Probability of attachment.
K	Boltzmann constant.
k	Mobility.
k	Abbreviation for kilo (10^3)
L	Mean free path.
M	Mass of an atom or molecule.
M	Abbreviation for million (10^6).
M_+	Mass of a positive ion.
m	Mass of an electron.

N Density of ions.

N^+ Density of positive ions.

N_{dE} Number of particles, out of a total of N, having energies between E and E + dE.

n Density of electrons.

p Pressure of the gas.

Q_{ex} Cross-section for excitation.

$Q_{elast.}$ Cross-section for elastic collisions.

Q_i Cross-section for ionizing collisions.

R Radius of the discharge tube.

R Resistance.

s Distance of separation of the parallel conductor transmission line.

T_e Electron temperature.

T_i Ion temperature.

T_g Gas temperature.

t Time.

V Volts.

V_a Applied potential.

V_b Breakdown potential.

v.p.m. Abbreviation for volume per million unit volumes.

X Applied field.

x x-Axis of co-ordinate system.

y y-Axis of co-ordinate system.

z z-Axis of co-ordinate system.

α First Townsend coefficient.

γ Second Townsend coefficient.

Δi Change in discharge current on exposure to light.

$-\Delta i$ Decrease in discharge current on exposure to light.

$+\Delta i$ Increase in discharge current on exposure to light.

$\%\Delta i$ Percentage change in discharge current on exposure to light.

δ Separation between striations.

i Discharge current.

i_D Discharge current in dark

i_L Discharge current under light.

i_+ Positive ion current.

λ Wavelength of electromagnetic waves.

μ Abbreviation for micro (10^{-6})

ν Frequency of electromagnetic waves.

ν_e Frequency of plasma-electronic oscillations.

ν_i Frequency of plasma-ionic oscillations.

π Ratio of the diameter of a circle to its circumference.

Σ Sign of summation.

LIST OF FIGURES AND ILLUSTRATIONS.

ABSTRACT

During the last ten years, experimental data have been obtained, mainly in Indian laboratories, about the effect of external irradiation by visible light on the current of an electrical discharge through certain electronegative gases. This effect is seen as a reduction (or in some cases, an enhancement) of the discharge current on exposure to visible light. Most of the previous work has been done on a.c. discharges, which favour the observations by showing a substantial reduction in the discharge current. However, since the different prccesses involved in an electrical discharge are better understood in the case of d.c. discharges, the present study was initiated with a view to obtaining experimental evidence in the case of a d.c. discharge, which may elucidate the primary processes responsible for the observed effect of visible light.

The experiments were conducted in air and hydrogen, which are known to exhibit the said light-effect; and the range of pressure had to be limited to low values so as to obtain conditions favourable to observe the effect. Special split-electrode geometry was used to observe separately the changes in the currents flowing along the walls and near the axis of the discharge tube. Two techniques were used to obtain the information about the constituent parameters of the discharge, in addition to measuring the effect of light on discharge current. A Langmuir probe was used to

investigate inside the discharge and the noise spectrum of the discharge was also studied in the range of 20-1000 Mc/s, using an external coupling.

The probe measurements were made in the plasma of the positive column of the discharge. Attempt was only made to measure the positive ion current to the probe, which showed a decrease in value on exposure to light. In view of the possibility of photo-dissociation of diatomic molecules into single atoms, a plausible explanation is advanced, supported by the observations of the effect of light on different parts of the currents, measured with the split electrode.

The noise spectrum from the discharge was found in a band of frequencies which could neither be related to plasma electronic oscillations nor to the plasma ionic oscillations. The observed noise seemed to be produced by a series of very narrow pulses at a repetition rate of a few kc/s. On exposure to light, the general trend was a diminution in the heights of these pulses and, in some cases, the lowering of the frequency of oscillations. The process of generating the observed signals is discussed in the light of their association with the different types of charged particles.

Results of an attempt to measure the time-lag of the irradiation effect by using brief pulses of light are given at the end; and a note on the conditions for formation of striations is included in the appendices.

CHAPTER I.

INTRODUCTION.

1.1 During the last ten years, a good amount of experimental data have been obtained, mainly in Indian laboratories, about the effect of external irradiation by visible light on the current of an electrical discharge through certain electronegative gases. Under suitable conditions this effect is seen, in most cases, as a reduction of the discharge current on exposure to visible light.

1.2 When electricity passes through a gas from one plane electrode, to another parallel to it, the phenomena taking place are many and complicated. At any point in the body of the discharge, ions are being produced by electron impacts, are disappearing by recombination, are diffusing away, and are being carried away by the electric field. These different processes, viz. ionisation of neutral particles, the non-uniform distribution of charged particles, and the attachment of charged particles to neutral particles had been the subjects of study, of many workers, since the beginning of this century.

1.3 The effect of external light and of impurities on the different processes occuring in a discharge tube were first studied by Thomson (1928) and later by Penning (1928 and 1932). In his study of the

effect of external light, Thomson observed that if the applied potential is slightly less than the break down potential (i.e. the potential at which a visible glow-discharge appears) and the discharge tube is exposed to light, the discharge takes place. This effect is also observed even if the metal electrodes are screened from irradiation or even in the electrodeless discharge. In Penning's experiments, in which the effect of neon illumination on a corona discharge in contaminated neon was studied, he was using the resonance frequency for the external irradiation and hence the observed reduction in the discharge current could be attributed to an increase in V_b, the breakdown potential.

1.4 In 1940, Joshi observed [Joshi & Narsimhrao (1940), Joshi & Deshmukh (1941)] that the r.m.s. value of the discharge current in a glass ozonizer, filled with chlorine at a pressure of about 10 cm. of Hg, and excited by an alternating potential, at a frequency of 50 c/s, decreased when the vessel was exposed to external visible light. If the irradiating source was removed, the value of the current was restored to its previous value. This differs fundamentally from Penning's observations in that it was observed with a range of irradiation frequencies which were quite different from the resonance frequency for the particular gas.

1.5 This reduction in discharge current on exposure to visible light was later observed in gases other than chlorine, such as oxygen, nitrogen, air, hydrogen; also in vapours of other halogens like bromine and iodine and in mercury vapour. It has been studied for various values of applied potential, gas pressure, intensity, frequency of irradiating sources etc., and the following are the principal conclusions reached:

1.5.1 (1) When V_a, the potential applied to the discharge tube is less than V_b, the breakdown potential, the discharge current increases due to the action of external light. [Such an increase in the discharge current due to light is denoted, henceforth, throughout the following text as $(+\Delta i)$.] When the applied potential is more than the breakdown potential, the discharge current decreases on exposure to external irradiation. [Such a decrease in the discharge current due to light is denoted, henceforth, throughout the following text as $(-\Delta i)$.] As V_a/V_b, the ratio of the applied potential to the breakdown potential is gradually increased, the magnitude of the decrease in current, $(-\Delta i)$, increases, reaches a maximum and then begins to decrease. In some cases, at large values of V_a, a small increase in $(-\Delta i)$ is again observed. [Prasad & Jain (1947), Mohanty & Kamath (1948a), Rao & Sharma (1949) and Deshmukh (1949a).] A typical curve

FIG. 1.

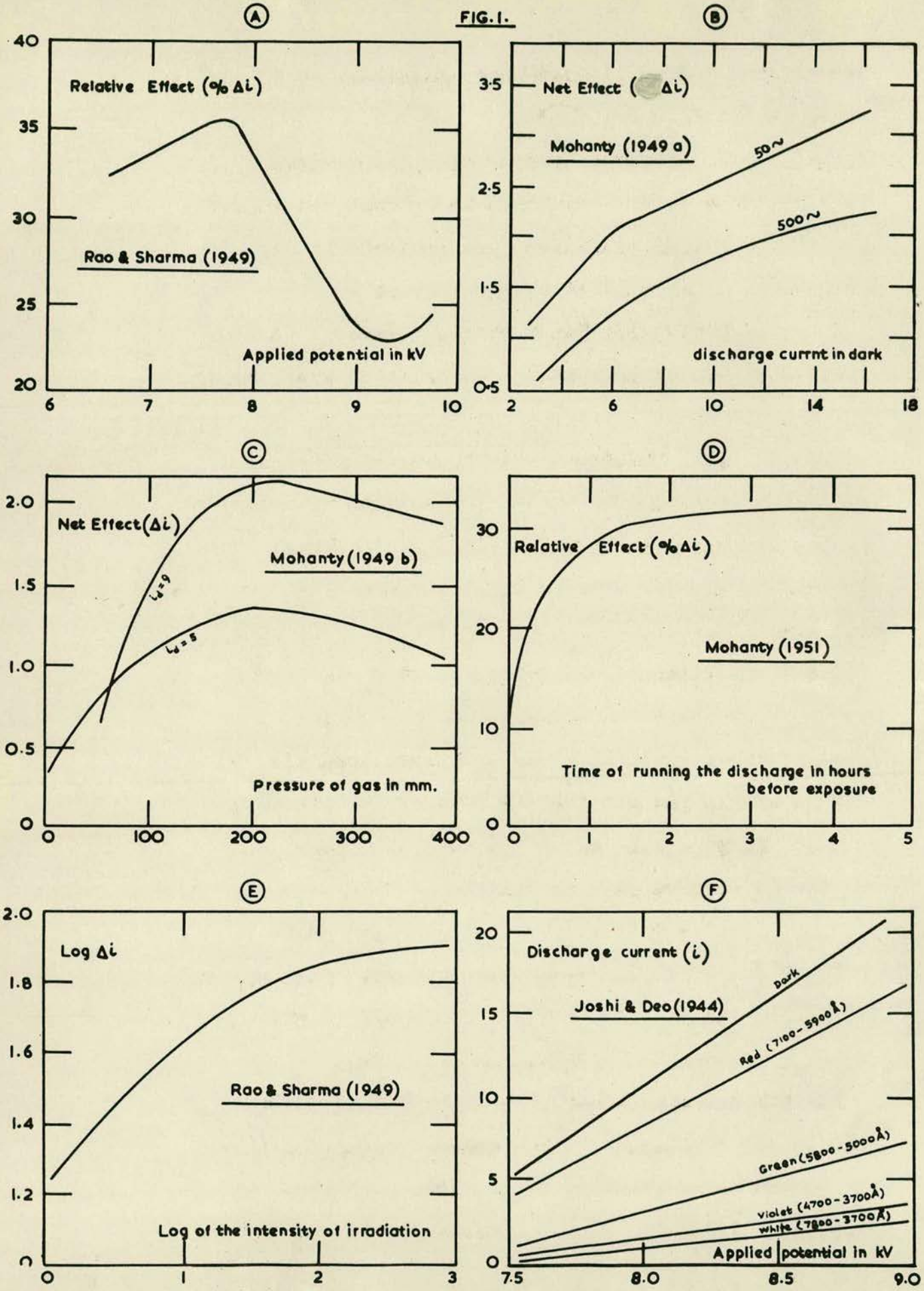
A
Relative Effect (% Δi)
Rao & Sharma (1949)
Applied potential in kV
40
35
30
25
20
6
7
8
9
10
B
Net Effect (Δi)
Mohanty (1949 a)
50~
500~
discharge currnt in dark
3·5
2·5
1·5
0·5
2
6
10
14
18
C
Net Effect (Δi)
Mohanty (1949 b)
Pressure of gas in mm.
2.0
1.5
1.0
0.5
0
100
200
300
400
D
Relative Effect (% Δi)
Mohanty (1951)
Time of running the discharge in hours before exposure
30
20
10
0
1
2
3
4
5
E
Log Δi
Rao & Sharma (1949)
Log of the intensity of irradiation
2.0
1.8
1.6
1.4
1.2
0
1
2
3
F
Discharge current (i)
Joshi & Deo (1944)
Dark
Red (7100 - 5900 Å)
Green (5800 - 5000 Å)
Violet (4700 - 3700 Å)
White (7800 - 3700 Å)
Applied potential in kV
20
15
10
5
0
7·5
8.0
8.5
9.0

summarising the above described dependence of (Δi) on V_a is shown in Fig. 1(A).

1.5.2 (2) In the case of a.c. discharges, the magnitude of the reduction in current, on exposure to visible light, decreases with increase in the frequency of the applied alternating potential. [Mohanty (1949a) and Rao & Sharma (1949).] A typical manner of this behaviour is shown graphically in Fig. 1(B).

1.5.3 (3) The magnitude of the reduction in current on exposure to light, is found to increase with p, the pressure of the gas inside the discharge tube. It reaches a maximum value and then falls with a further increase in pressure. [Jobhi & Deo (1944a), Mohanty (1949b) and Vishwanathan (1949),] The critical pressure at which the maximum effect of light is observed in a particular case, depends upon the nature of the gas and the geometry of the discharge tube. In Fig. 1(C) is illustrated this behaviour of ($-\Delta i$) with respect to p.

1.5.4 (4) The magnitude of the diminution in current is also observed to be dependent upon "ageing", i.e. upon the time for which a discharge is allowed to run, before the observations are taken. [Mallikarjunappa (1948), Deshmukh & Dhar (1949b) and Mohanty (1951).] The general mature of this influence is as shown in Fig. 1 (D).

1.5.5 (5) The observed effect of the variation

in the intensity of the irradiating source on $(-\Delta i)$ is as shown in Fig. 1(E). The magnitude of the effect first increases with intensity and then reaches a saturation value. [Joshi & Deo (1943), Mohanty & Kamath (1948b) and Rao & Sharma (1949).]

1.5.6 (6) When one uses different wavelengths for the external irradiation, the effect appears to decrease with wavelength as is shown by a typical example in Fig. 1(F). [Deo (1944), Joshi & Deo (1944a) and Mohanty & Kamath (1948b).] Canac et al (1950) have recently reported a similar effect using extremely short wavelengths.

1.6 Most of the previous work, which is summarised above, has been done with discharges excited by an alternating potential difference and although attempts have been made to advance explanations to account for the observations, several points of dispute arise when a unification to form a theory is pursued. This is, perhaps, partly due to the fact that the theory of the a.c. discharges is not fully developed because of a lack of accurate measurements of the fundamental parameters of a discharge, which are often complicated by alternating potentials. Thus, although numerous measurements have been reported, since their relation to the known parameters of the discharge was, in most cases, indirect, the available information has not been adequate in many respects.

1.7 The present work was, therefore, initiated with a view to make experimental observations under simple conditions found in a d.c. discharge. Use can then be made of the better formulated theories of d.c. discharges for elucidating the primary processes responsible for the observed effect of light. Some of the methods employed for measurements are original and are not known to have been used in any previous work on the subject. The better knowledge about the various processes that could be expected in simpler conditions of d.c. discharges was thought to be a definite advantage. Further with the more direct way of investigation inside the discharge by a probe, more specific significance could be attached to the observations as well as the inferences derived therefrom. It was also hoped that a comparison of these with the already known facts might be useful to test the validity of explanations relating to the cases of a.c. discharges.

1.8 In an electrical discharge through a gas, the magnitude of the discharge current is determined by the number of charged particles arriving at the electrodes per unit time. This we can write as:

$$i = \sum n e k X \qquad \text{- - - - - (1.8.1)}$$

where i is the discharge current

n is the number of charged particles carrying a charge e,

k is the mobility

and X is the externally applied field under which the charged particles are moving.

The sign, sigma (Σ) denotes the summation of all the individual contributions by the different kinds of charged particles, namely electrons, positive ions and negative ions. If a change in i occurs, it could be expected to be associated with a change in one or all the parameters of the right hand side of equation (1.8.1). The external irradiation by visible light has obviously no effect on the values of either e or X, once the discharge is struck. Therefore, a change in i should be referable to either a change in n or k or both.

1.9 Change in n:

The field distribution and the ion and electron concentrations are different in different regions of the discharge tube. The magnitude of the effect of external irradiation by visible light could, therefore, be expected to vary in these different regions of the discharge. Agashe (1951) has shown that the maximum effect is observed in those portions of the discharge tube where the glow of the positive column appears. The positive column contains ions, both positive and negative, and electrons. Because of the lighter mass and hence greater velocity of the electrons, the current in the positive column of a

discharge is mainly due to the motion of electrons. A decrease in the discharge current on exposure of the positive column of the discharge to external visible light could, therefore, mean a decrease in n, the number of free electrons.

1.9.1 Thomson & Thomson (1933, p. 374) has given the various causes for the loss of electrons in the positive column. They are: (a) Recombination of electrons with positive ions to form neutral molecules or atoms, (b) side-diffusion of the electrons to the walls of the discharge tube and (c) loss of electrons by way of their attachment to form negative ions. The possibility of a modification in these processes, responsible for loss of electrons by the action of external irradiation could be examined in further detail:

1.9.2 (a) The process of recombination of positive and negative particles is known to be almost negligible in the case of glow discharges. Compton et al (1924) have reported that the luminosity of the positive column results from the process of readjustment within the atoms or from partial ionization only. Thus any appreciable increase in the loss of electrons due to more recombination under light, seems to be very improbable.

1.9.3 (b) The rate of side-diffusion of electrons is related to the temperature of the gas and any change in the diffusion rate would manifest itself

with a corresponding change in the temperature of the gas. The intensity of the source of the external irradiation is far too low to warrant any significant rise in the temperature. Minute changes in pressure, observed under irradiation, are also too sudden to be attributed to a change in the temperature of the body of the gas. [Agashe (1952)].

1.9.4 (c) In the positive column of a gas discharge, electrons could also be lost by their attachment to neutral particles, to form negative ions. This attachment depends upon the 'electron affinity' of the particular gas. Thomson (1916), Massey & Smith (1936) and Smyth (1931) have studied the equation of attachment of electrons to neutral molecules. The main three influencing factors are (i) the nature of the gas, (ii) the collisional frequency of electrons and (iii) the energy of electrons.

1.9.4(a) (i) <u>The nature of the gas</u>: In the study of attachment in various gases, it was first found that electrons will not attach in helium, neon, nitrogen and hydrogen, if these gases are pure; while they will do so in oxygen, sulphur dioxide, chlorine and hydrochloric acid gas. More recent observations [Branscomb & Fite (1954)] have experimentally established the identity of negative ions formed in hydrogen discharge also. The attachment of electrons to chlorine or hydrochloric acid gas molecules is believed to be preceded by their dis-

sociation into Cl^+ and Cl^- or H^+ and Cl^- . Wahlin (1922) reports that, in general, electrons attach more readily to dissociated fragments. It is to be noted that the influence of external irradiation by visible light is mostly observed in diatomic molecules like H_2, N_2, O_2, Cl_2, Br_2, I_2 etc. Hudson et al (1930) have said that when adsorped oxygen and water vapour came out to contaminate a tube filled with argon, negative ions were found to be formed readily. Deshmukh (1947), in his study of the effect of external visible light on different gases, gives their order, according to the amount of effect they show, under similar conditions, as $H_2 < N_2 < Air < O_2$ and the electron affinity of these gases varies precisely in the same order.

1.9.4 (b) (ii) <u>The collisional frequency of electrons</u>: This second factor influencing the attachment of electrons to neutral particles forming negative ions, obeys the gas-kinetic laws. A change in this factor would naturally be associated with a corresponding change in the pressure or temperature of the gas. The plausibility of modification by external irradiation is therefore similar to the one as discussed already in 1.9.3.

1.9.4 (c) (iii) <u>The energy of electrons:</u> The electron attachment is also governed by the average energy of electrons, which in turn depends on the distribution of electron energies in the body of the

gas. According to the laws deduced by Maxwell, which deal with the case known as the Maxwellian distribution of energies, the distribution function is given by (cited by Loeb (1947), p. 653)

$$N_{dE} = \frac{2N\sqrt{E}}{(\pi)^{1/2}\,(kT)^{3/2}} \cdot \varepsilon^{-E/kT} \cdot dE \quad ---(1.9.1)$$

where N_{dE} is the number of particles out of a total of N, which have the energies between E and (E + dE)

and kT represents the kinetic energy of the particle.

The average distance, $\bar{d}$, which an electron moves in a field X, before attaching to a neutral molecule is

$$\bar{d} = k_e n X t \quad ---------(1.9.2)$$

where n is the average number of impacts with gas molecules before an electron can attach

k_e is the electron mobility

and t is the time an electron spends between impacts*.

1.9.5 Thus the probability of attachment of electrons to neutral molecules depends upon X/p. From their experiments for the determination of the probability of attachment of electrons as a function of X/p, for various gases, Bloch & Bradbury (1935) have plotted a relation between the average electron energy and the variation of the probability of

---

*The quantity t may be evaluated from the ratio of the mean free path to the velocity of agitation ($L/\bar{c}$) which is related to k_e, by the Townsend's equation $k_e = \frac{0.815}{300} \cdot \frac{e}{m} \left(\frac{L}{\bar{c}}\right)$.

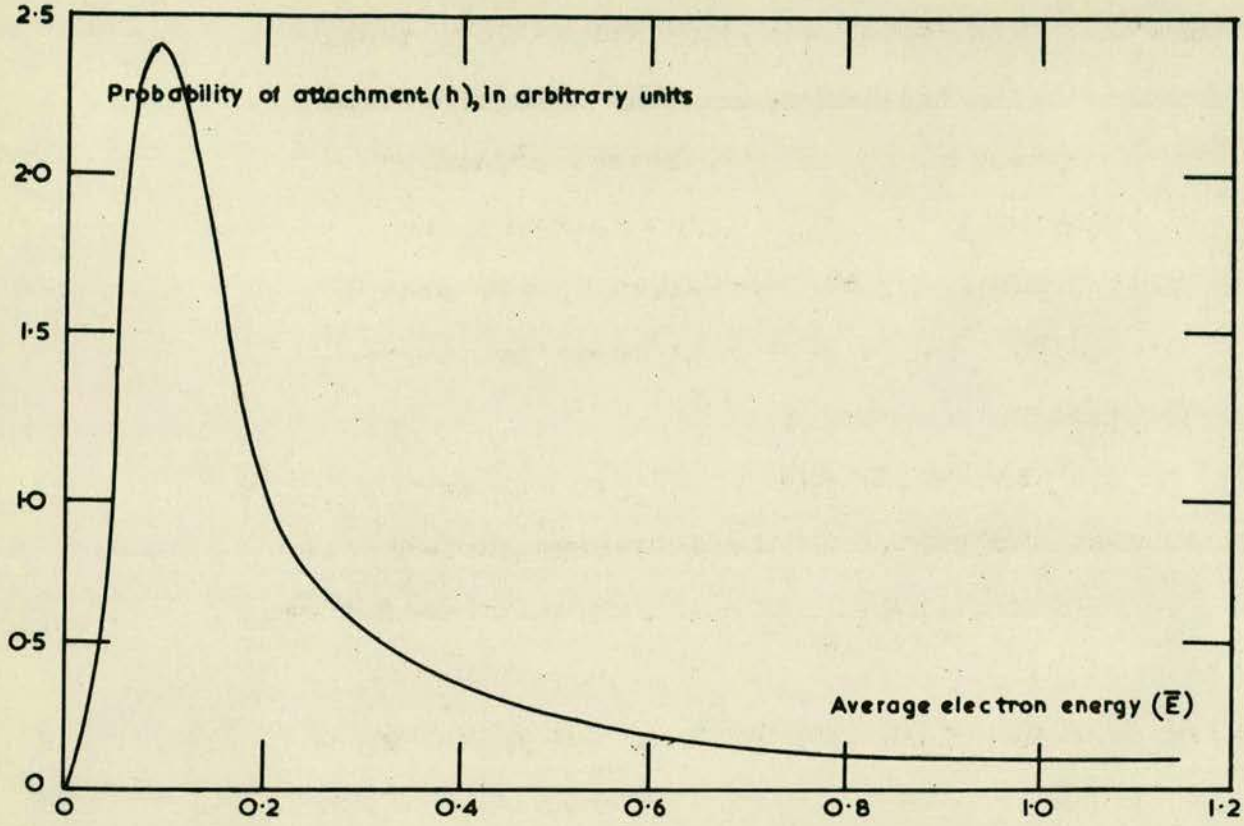
2·5
2·0
1·5
1·0
0·5
0
Probability of attachment (h), in arbitrary units
Average electron energy ($\bar{E}$)
0
0·2
0·4
0·6
0·8
1·0
1·2

FIG. 2A.

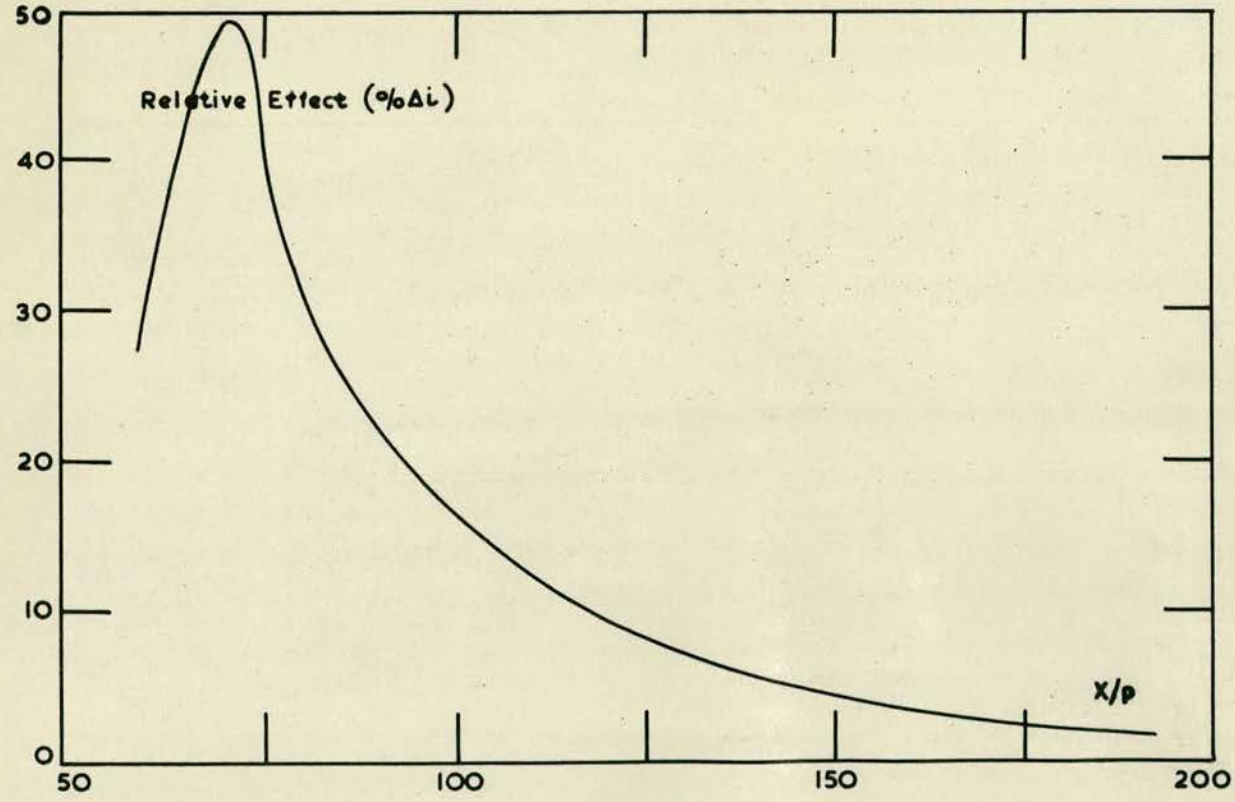
50
40
30
20
10
0
Relative Effect (%Δi)
X/p
50
100
150
200

FIG. 2 B.

attachment. This curve is reproduced in Fig. 2(A). From the results published by Mohanty & Kamath (1948b) giving the dependence of the percentage effect† of external light on V_a and p, a curve is drawn, as shown in Fig. 2(B), for the variation of percentage effect with X/p. It is seen that these two curves are quite similar in nature.

1.9.6 All this evidence, therefore, strongly suggests that the change in the discharge current due to external visible irradiation is likely to be due to a change in n, the number of free electrons in the body of gas. This change in n is probably due to the loss of electrons mainly because of their attachment to neutral molecules to form negative ions.

1.10 Change in k:

The right hand side of equation (1.8.1) contains another factor, with which the influence of external light could be associated. This is the mobility term k. Such a possibility of a change in the mobility of charged particles has been discussed by Agashe (1952). By following a method similar to the one by Chattock (1899 and 1909) in which simultaneous measurements of the changes in the discharge current and in the pressure of the gas were made, he concludes

---

† The percent light effect (denoted also in figs 1(A) and 1(D)) is calculated as follows. If, the original discharge current (in dark) i_D reduces to i_L on exposure to light, the net effect is $i_D - i_L$ $(= -\Delta i)$, and the percentage effect is $[(i_D - i_L)/i_D] \times 100$ $(= \% \Delta i)$.

that there is a reduction in the average mobility of charged particles. According to Langevin's theory of mobility

$$k \propto (M)^{-\frac{1}{2}} \quad ----- (1.10.1)$$

where M is the mass of the charged particle. Therefore, a reduction in the average mobility under external irradiation could mean an increase in the average mass of the charged particles. This may happen when more ions are formed by external irradiation. The electrons moving under the influence of the applied external field can bring about ionization in two ways. They can produce positive ions by knocking out the electrons from neutral molecules with the energy acquired by their velocities, or they can attach to neutral molecules to form negative ions.

1.10.1 For formation of a greater number of positive ions by electron impact under external light, the electrons should acquire additional energy for increased ionization by collision or some extra electrons of sufficient energy of ionization should be present under external irradiation by visible light. A greater number of negative ions, on the other hand, could be formed under light if the factors responsible for their attachment to neutral molecules are influenced by the external light, as discussed earlier.

1.10.2 Since the frequency of the visible light

used for external irradiation is quite different from the resonance frequency of the gas, any mechanism by which the electrons could acquire additional energy from the external light to form more positive ions, cannot be conceived. Formation of negative ions, therefore, appears to be reasonably responsible. Whether the external light favours the attachment of only the available electrons or more electrons are given out by some kind of photoelectric action which attach to neutral molecules forming negative ions, is the question to which the available literature on the subject, seems to provide no satisfactory answer.

1.11 The present investigation was, therefore, planned to obtain direct evidence of establishing the process of formation of the negative ions. Mass spectrometric analysis was considered, but the designing and setting up of such suitable experiments (as discussed later in 4.1.2), specially for these observations, based on rather a speculative theory, was not possible within the available conditions and resources. In spite of its limitations, the Langmuir method of investigations by a probe was, therefore, adopted, because of its simplicity of instrumentation.

1.12 The previous experimental data on the subject using a.c. discharges has been, in many cases,

supplemented by the study of the high-frequency oscillations generated by the discharge. [Joshi (1944b) and Harries & Engel (1951).] High frequency oscillations have also been previously observed by many workers in the case of d.c. discharges. [Appleton & West (1923), Tonks & Langmuir (1929a), Cobine & Gallagher (1947 a and b) and Armstrong, Emeléus & Neill (1951).] Since these oscillations are associated with the movements and concentrations of charged particles in the discharge, this technique was also employed in the present study to get additional information which may corroborate the probe measurements.

CHAPTER II.

THEORETICAL SURVEY OF THE PHYSICS OF THE GLOW DISCHARGES.

2.1 The expression 'Electrical Discharge' for a flow of electricity in a gas was probably derived from early experiments of Coulomb wherein he showed that a charged electroscope is caused to 'discharge' by a certain process. Later, during his investigations about low pressure discharges, Faraday introduced a term 'glow discharge', to distinguish it from the other two main types of continuous discharges, namely 'dark discharge' and 'an arc discharge'. Following the discovery of X-rays by Röntgen in 1895 and of the electron by J. J. Thomson in 1896, a detailed quantitative work was initiated for the study of the mechanism of gas discharges where the electrical, optical and the associated chemical properties of the discharge are expressed in terms of atomic data like charge, mass, mean free path, dielectric constant, gas pressure, temperature etc. and sometimes the geometry of the discharge vessel.

2.2 AVERAGE PROCESSES: The mechanism of the discharge is governed by certain average processes, among which are:

(1) The mobilities of charged particles which are related to the applied electrical field.

(2) The energy distribution or the variation in energy among the number of particle population in a discharge, and

(3) The first and second Townsend Coefficients (α and γ) for the ionization of the gas and for production of secondary electrons.

The role of the first two processes, in the present study, has already been discussed earlier in 1.10 and 1.9.4(c) respectively. The mechanism of the two Townsend Coefficients is closely related to the individual processes occurring in a discharge, and is discussed in detail below.

2.3 INDIVIDUAL PROCESSES: Of all the individual processes associated with a glow discharge, ionization is the most vital one for the self-maintenance of the discharge. This mechanism of production of new electrons is associated to the process of ionization by collision. At any point in the body of the discharge, electrons, ions and neutral gas particles - both in excited and ground state - are simultaneously present. Each of them is, therefore, responsible for the process of ionization.

2.4 Ionization by electron collision: Electrons, while moving under the applied field, can have three types of collisions. (a) elastic collisions, (b) exciting collisions and (c) ionizing collisions. The total cross-section of collisions by electrons

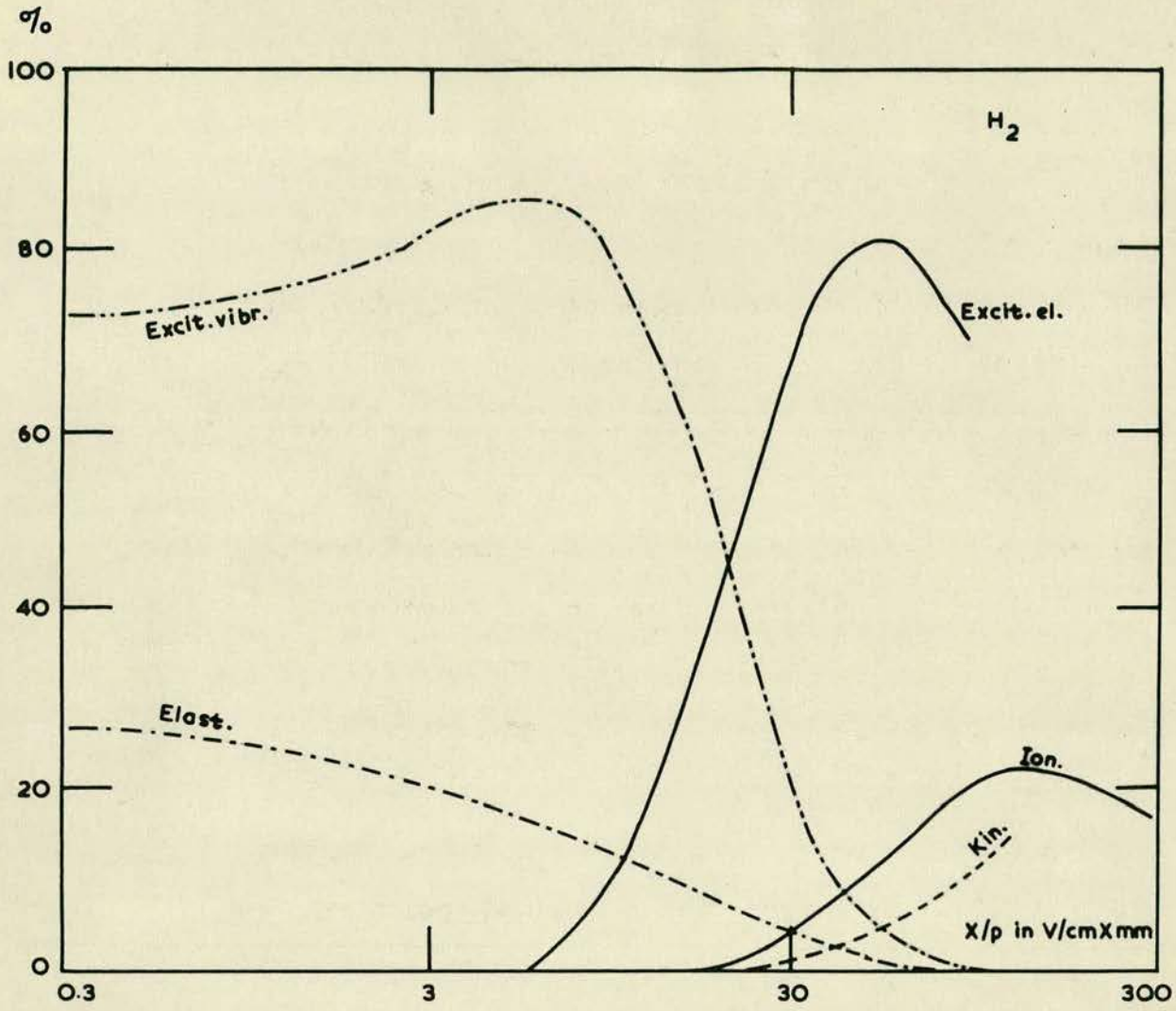

Fraction of the total energy received by the electrons from the electric field which is spent in elastic collisions (Elast.), excitation of electronic level (Excit. el.), excitation of vibrational levels (Excit. vib.), ionization (Ion.) and increase of kinetic energy of electrons (Kin.).

FIG. 3.

is, thus, the sum of all these three different types. The relative percentage of these processes in the case of H_2 is shown in Fig. 3 as is given by Penning (1938).

2.4.1 (a) Elastic Collisions: When electrons are moving in a swarm of gas molecules, depending upon the value of the mean free path, which in turn is governed by the pressure of the gas, they suffer collisions with gas molecules. For all energies below excitation or ionization potentials, such collisions are known as elastic collisions wherein the energy of the electron remains substantially unchanged. This follows from the fact that since the mass of the gas molecule is large compared with that of an electron, the energy loss, as required by the laws of conservation of energy and momentum, is insignificant. From the electrical point of view, such collisions are, therefore, of little importance.

2.4.2 (b) Excitation Collisions: The process of excitation collision can be denoted by

$$A + e \rightarrow A^* + e$$

where A is the normal atom, e the electron and A^* the excited atom. The probability of excitation, which is the ratio of the cross-section of excitation to the kinetic theory cross-section, depends on the electron velocity. It is zero at the excitation potential and rises to a maximum value lying generally between 0.001 and 0.1 at a small voltage above the exciting potential. Thereafter, it is

known to fall gradually. In the case of hydrogen, the relative probability of excitation collision is 33.5 for the incident electrons of an energy of 100 eV and rises to a value of 45.3 for 1000 eV electrons. The ionization and excitation cross-sections for various transitions of hydrogen are given in Appendix D.

2.4.3 (c) Ionizing Collision: This type of collision is denoted symbolically by

$$A + e \rightarrow A^{+} + e + e$$

where A^{+} is the positive ion of gas A. The cross-section of ionization is again zero at the ionizing potential, increases to a maximum and then slowly begins to decrease. In the case of atomic hydrogen the maximum cross-section for ionization is about 275.2×10^{-16} cm^2 for electron energy of 112 eV, while the corresponding figure for molecular hydrogen is 1.01×10^{-16} cm^2 for electron energy of 70 eV. The probability of ionization, which is dependent on the electron energy has a maximum value generally greater than the corresponding quantity in excitation.

2.5 <u>Ionization by positive ion collisions</u>: When electrons collide with neutral gas particles in a discharge, they form positive ions, which are drawn towards the electrodes, under the action of the externally applied electric field. These positive ions themselves can sometimes cause further ionization by impact. The mean free path of positive ions is $4\sqrt{2}$ times that of electrons and hence their total

collision cross-section is correspondingly higher. As a result of this higher frequency of collision, together with their greater mass, the positive ions can only acquire energies much less in comparison to the electron energies. This reduces the chances of further ionizing collisions of positive ions with neutral gas molecules to a rarity.

2.5.1 Positive ions can suffer another type of change in their energies by recombination in which the liberated energy can appear either as a kinetic energy of a three-body collision or as an emission of a quantum of radiation.

2.5.1(a) The walls of the discharge vessel are very efficient in favouring the three-body collisions. Hence, in conditions where the mean free path of positive ions is comparable in magnitude to the dimensions of the discharge vessel, this process is believed to be important. Most of the previous work on the study of the effect of external visible light on glow discharges had been done with alternating potentials using ozonizers for discharge vessels. The discharge was, therefore, confined in annular spaces of small widths and the importance of the dependence of wall processes on the observation can, therefore, be readily realised.

2.5.1(b) In the radiative recombination process, there can be an emission of radiation of any wavelength up to a maximum wave number. This can symbolically

be written as

$$A^+ + e \rightarrow A + h\nu \ .$$

$$\text{or} \quad A^+ + B^- \rightarrow AB + h\nu .$$

where e is an electron and B^- is a negative ion. The emitted wavelength may be very short to have its own after-effects as mentioned later in 2.6. In the process of recombination, an electron can combine with its parent ion or with another positive ion. The former has been termed by Loeb (1947, p. 87) as 'preferential recombination' and the latter as 'volume recombination'. Quantitative experimental work on radiative electron-ion recombination is rare and hence the relative importance of the above two processes of positive ion annihilation, which in a particular glow discharge depends upon the nature and the geometry of the gas column between the two electrodes, is difficult to assess.

2.6 Radiation may also be produced inside a discharge by the return of excited atoms to lower or ground states, i.e.

$$A^* \rightarrow A + h\nu$$

This radiation may be of a sufficiently short wave length to ionize those impurities in the gas, which have lower excitation and ionization potentials. Alternatively, this radiation can have a photo-electric action on the cathode to produce secondary electrons. In the present study, most of the impurities in hydro-

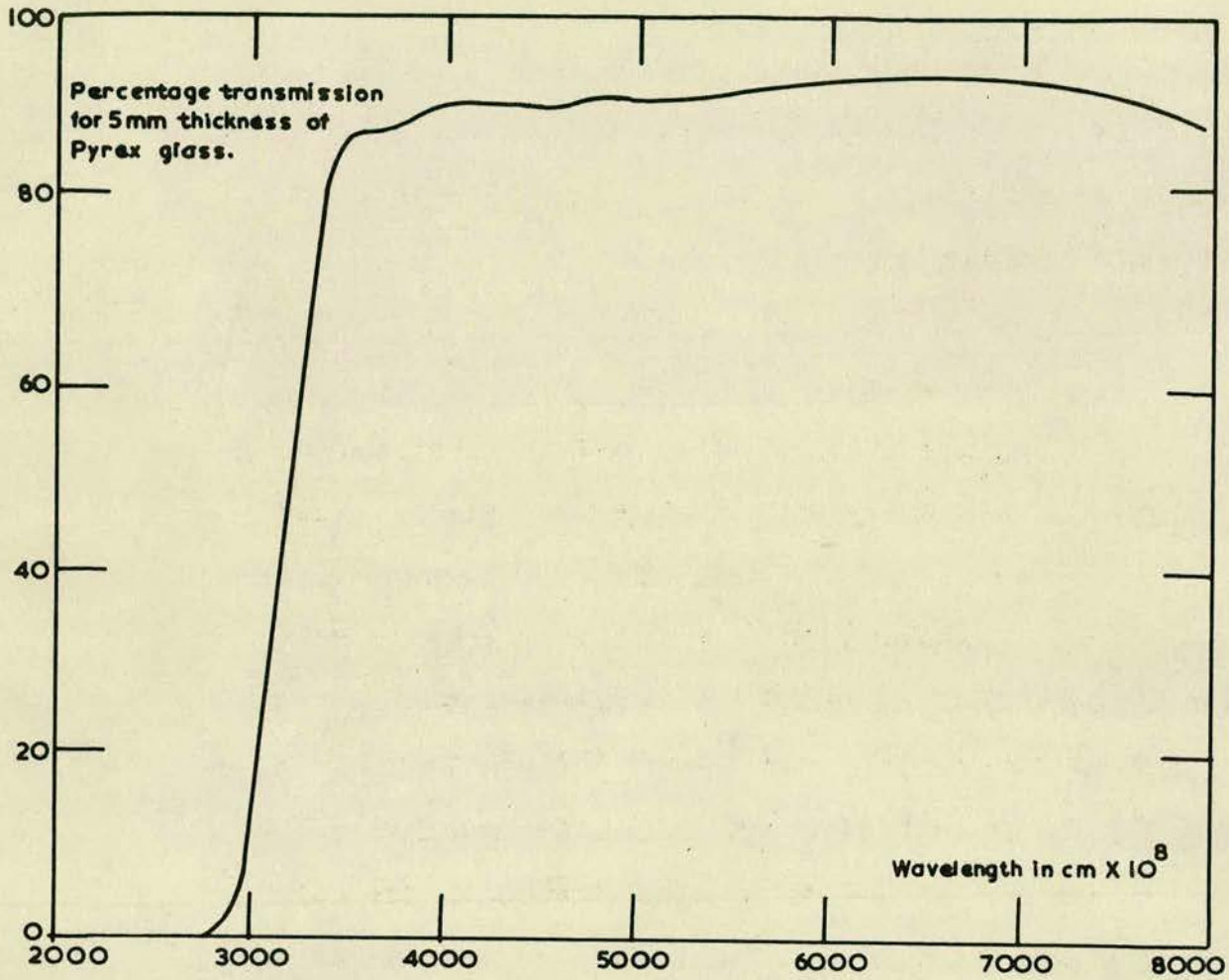
100
80
60
40
20
0
Percentage transmission for 5mm thickness of Pyrex glass.
Wavelength in cm X 10^8
2000
3000
4000
5000
6000
7000
8000

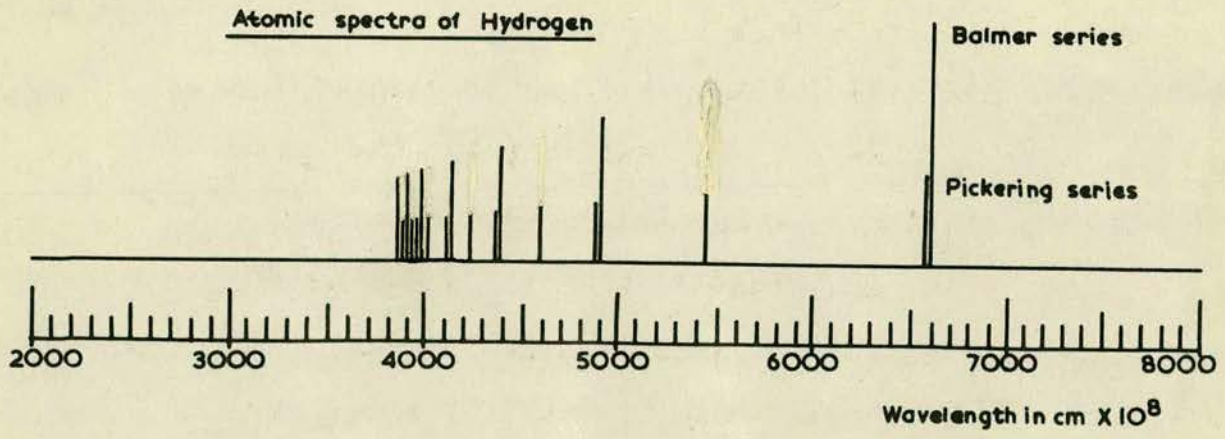
Atomic spectra of Hydrogen
Balmer series
Pickering series
2000
3000
4000
5000
6000
7000
8000
Wavelength in cm X 10^8

FIG.4.

gen as given in 3·3·4, except oxygen, had ionizing potentials higher than that of hydrogen (vide Appendix C).

2.7 Another individual process in a discharge, which is of particular interest when studying the effect of external irradiation, is photo-excitation or photo ionization.

$$A + h\nu \rightarrow A^*$$

$$\text{or } A + h\nu \rightarrow A^+ + e$$

The first, i.e. excitation by a photon is an unlikely process, unless the photon energy is close in value to the excitation potential. The discharge vessels used in the present study were made of pyrex glass, which has a cut-off value for transmission at a wavelength of about 2500×10^{-8} cm, as shown in Fig. 4. The series of line spectra of atomic hydrogen are also shown at the bottom of this figure on the same scale of wavelengths. The most part of the maximum intensity of the continuous spectrum of molecular hydrogen, which falls at a wavelength of about 2600×10^{-8} cm. lies outside the relative transmission curve for pyrex glass. The latter process of photo ionization, which is the converse of electron-ion recombination, is doubtless similar in character to photo-electric effect and such phenomena as the exciting of H/F currents in conductors by electric waves and the polarization of dielectric media, when

traversed by electric waves. Massey, (1950) gives an absorption cross-section for H, at the spectral limit, of 0.6×10^{-17} cm^2 .

2.8 In the general ionization process, metastable atoms play an important role. In a metastable state the valency electron of an atom moves in an orbit, whose energy is greater than that of the normal orbit, but a reversion from this orbit to the normal with an emission of radiation is forbidden by the selection principles. The length of time for which the atom persists in a metastable state will presumably be longer than for the ordinary excited state, for the ordinary state is terminated by the emission of a quantum of radiation, a process which is usually determined by the internal mechanics of the atom. The energy of the metastable state, however, cannot escape from the atom without the co-operation of some external agent. The life-time of a metastable atom is, therefore, usually greater than that of a normal excited state, by a factor of about eight. Moreover, the electrically neutral state of the metastable atoms enable them to penetrate in different remote regions of the discharge.

2.8.1 Metastable atoms may gain an additional energy by collision, which would first raise them to a normal excited state, and then allow them to return to the ground state by emission of a quantum of radiation. When an electron of mass m collides with

another particle of mass M, the frictional loss in its energy is 2.66(m/M). In the case of Hydrogen the mass ratio of an hydrogen atom to an electron has a value = 1837.5. Hence, the additional energy which a metastable atom could gain in its collision with an electron is only 0.001447.

2.8.2 A metastable atom can ultimately diffuse to the cathode and if sufficiently energetic, it can produce secondary electrons. However, if there are impurities present in the gas, which have energies of ionization less than that of the metastable atoms, the metastable states of the atoms are destroyed much sooner before they have any chance of falling on the cathode and producing secondary electrons. The variation in the voltage-current characteristic of glow discharges, when irradiated by 'resonance' frequencies, is also due to the metastable atoms present in a discharge. Irradiation by strongly absorbed radiation diminishes the concentration of metastable atoms, removing them as sources of secondary ionization. By using filters for absorbing lines in the case of Helium, Meissner & Miller (1952) have proved that observed effect was explicable by considering the possible transitions involved.

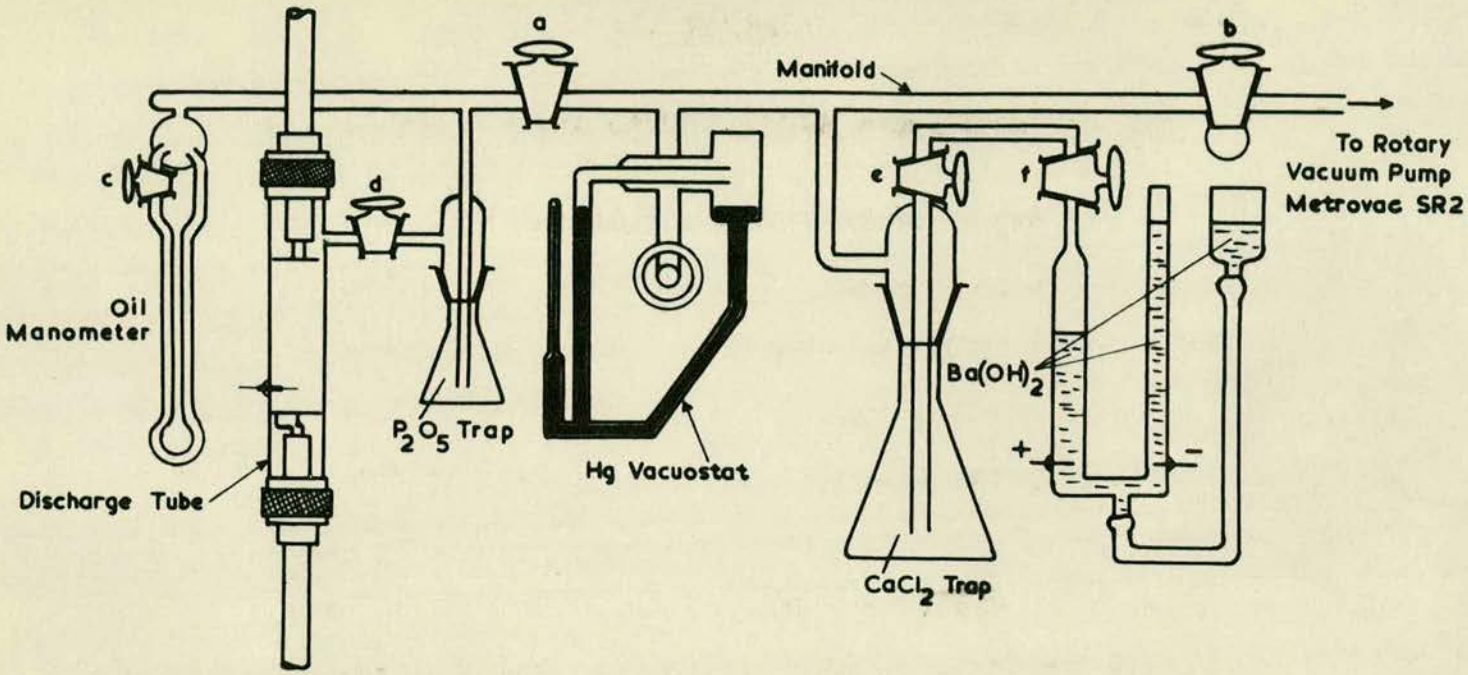
a
b
Manifold
To Rotary
Vacuum Pump
Metrovac SR2
c
d
e
f
Oil
Manometer
P_2O_5 Trap
Hg Vacuostat
$Ba(OH)_2$
+
−
Discharge Tube
$CaCl_2$ Trap

FIG. 5.

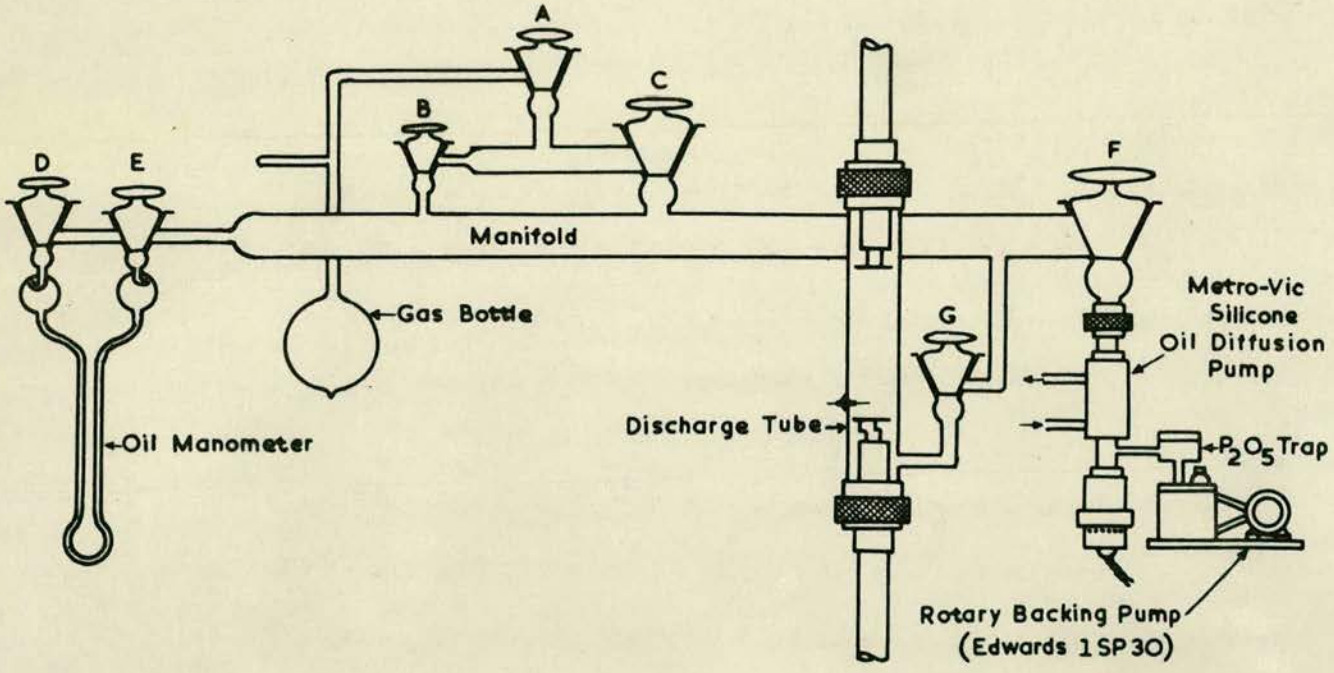
A
B
C
D
E
F
G
Manifold
Gas Bottle
Oil Manometer
Discharge Tube
Metro-Vic
Silicone
Oil Diffusion
Pump
P_2O_5 Trap
Rotary Backing Pump
(Edwards 1SP30)

FIG. 6.

CHAPTER III

THE APPARATUS AND EXPERIMENTAL ARRANGEMENTS.

3.1 The experiments were carried out with two different vacuum systems, A and B which are shown schematically in Figs. 5 and 6. The experiments in the case of discharges in air were carried out on the vacuum system A, shown in Fig. 5; and it was originally intended to carry out the experiments with hydrogen also with the same system. However, as discussed later in 3.2.6, the latter half of the experiments with hydrogen were subsequently performed using the vacuum system B as shown in Fig. 6. This second system was essentially the same in nature as the first one, with an additional advantage of obtaining a better purity of the gas.

3.2 VACUUM SYSTEM A: This vacuum system, shown schematically in Fig. 5, was made entirely in Pyrex glass. The main horizontal manifold of this system, carrying two stop-cocks 'a' and 'b', was connected at one end to a "Metrovac"† rotary vacuum pump of the type SR2, which also incorporated a phosphorus pentoxide trap, beyond stop-cock 'b', in addition to the one shown near the discharge tube in Fig. 5. At the other end of the manifold was an oil-manometer. The discharge tube was joined to the manifold in between the oil-manometer and the stop-cock 'a', via

---

† Metropolitan Vickers Co. Ltd., (Manchester, England)

a phosphorus pentoxide trap. The stop-cock 'd' could isolate the discharge tube from the entire vacuum system. Two other side-tubes, joined to the manifold in between the stop-cocks 'a' and 'b', were connected to a mercury manometer and to another drying trap of calcium chloride.

3.2.1 The Oil-manometer. The oil-manometer used on the system was made of a Pyrex U-tube with a single large spherical bulb in between the limbs and the manifold, to prevent any accidental rise of the oil into the manifold. With the stop-cock 'c', the left-hand limb could be isolated from the right-hand limb, which was always in contact with the manifold. "Apiezon† oil B" was used as a fluid for the manometer. The vapour pressure of this oil is 10^{-7} mm.Hg. at room temperature. The specific gravity of Apiezon oil B was 0.868 at 20° C. With the value of the specific gravity of mercury at the same temperature as 13.5458, the magnification ratio was found to be 15.61. Thus a difference of 15.61 mm. between the levels of the oil in the two limbs of the manometer would indicate a difference of pressure of 1 mm. of mercury. From some preliminary experiments for the calibration of the bore of the manometer limbs, it was found that the central parts of the two limbs, which would be used for the pressure measurements were identical in bore to better than one per cent. The manometer was, therefore,

---

† Shell Chemicals (London) Ltd. Sole Agents: W. Edwards and Co. (London) Ltd.

used by reading the difference between the oil level in the left-hand limb only, from its zero position. A scale was made of "Perspex"† to read the pressures directly in mm. of mercury. On this scale, a length of about 155 mm. was engraved with equal divisions, (having longer strokes to distinguish every fifth and tenth division) such that every 39 millimeters of its length were subdivided into 50 equal divisions. Each of this engraved division on the scale, which was now equal to 0.78 mm, was used to read a pressure difference equal to 0.1 mm. of mercury. Since the actual magnification ratio (as given earlier) was 15.61, the exact half-ratio, for use when reading one limb only, would be 0.7805 instead of 0.7800. This introduces an error of [1 - (0.78/0.7805)=] 0.00064 mm. per mm of mercury in the measurements of the gas pressure. With the help of a magnifying glass of a focal length of about 60 mm, to read the oil-level inside the limbs of the manometer, an accuracy of 0.05 mm. of mercury could be obtained in the pressure measurements made on the manometer.

3.2.2 <u>The Mercury Manometer</u>: This was an all-glass "Edwards" Vacustat‡" which is a miniature McLeod gauge. The range of the instrument for pressure

---

†Regd. Trade name of I.C.I. Industries Ltd. (England)

‡Regd. Trade mark of W. Edwards and Co. (London) Ltd.

measurement was 0 - 10 mm. of mercury. It was mounted on a B12 ground-glass cone, attached to the manifold. This gauge was used only in the preliminary stages of the experiment, mainly to measure the absolute degree of ultimate vacuum attainable on the system and to get an idea of the pressure of the gas, generated by electrolysis, which could be stored in the calcium chloride trap. (see 3.2.4). In order to eliminate mercury vapour contaminations, while making final observations, the Vacustat was taken out of the ground-glass core and a blind B12 male glass cone was substituted instead.

3.2.3 The Drying Traps: Both the traps, one containing phosphorus pentoxide and the other calcium chloride, used for drying the gas, were made from flat-bottom Pyrex bottles with ground-glass cone joints, as shown in Fig. 5. With this arrangement, the drying agents could be renewed as frequently as necessary.

3.2.4 The Gas-generating system: When this vacuum system was first designed and assembled, it was intended to carry out the experiments with hydrogen also on the same set-up. For this purpose, an apparatus was made (as shown on the right-hand-side of Fig. 5) for preparing hydrogen by electrolysis. A Pyrex U-tube, in which two platinum electrodes were sealed near the U-bend, was connected by a short

length of rubber tubing to a reservoir, which could be raised or lowered in height. The end of one of the two arms of the U-tube was open while the other was connected to a calcium chloride trap via two stop-cocks 'e' and 'f'. Hydrogen was generated by electrolysis of 1/15 normal solution of Barium Hydroxide $[Ba(OH)_2]$ placed in the U-tube. The electrode in the left arm which carried the stop-cock 'f' was made positive.

The procedure of generating and storing the gas was as follows: When the manifold of the sytem was open to the atmosphere, both the stop-cocks 'e' and 'f' were opened and the reservoir carrying the barium hydroxide solution was raised until all the air between the stop-cock 'f' and the level of the solution in the left-arm of the U-tube was expelled into the manifold. The stopcock 'f' was then closed and the manifold, together with the calcium chloride trap, was evacuated. The degree of vacuum attained could be measured with the Vacustat. There was a second phosphorus pentoxide trap in between the stop-cock 'b' and the rotary pump, as mentioned earlier in 3.2, to remove all water vapour. The out-gassing of the system was carried out by a prolonged treatment of a H/F discharge at about 20 kc/s obtained from an "Edwards Tesvac†", model T1.

While the system was being evacuated and outgassed, (with all the stop-cocks, except 'f', open) the barium hydroxide solution in the U-tube was electrolysed, by

---

†W. Edwards and Co. (London) Ltd.

applying a steady potential difference of about 20 volts between the two platinum electrodes in the U-tube , the electrode in the left-arm being made positive. On electrolysis, the barium hydroxide solution decomposed into hydrogen and oxygen. The oxygen evolved in the right-arm of the U-tube was allowed to escape into the atmosphere, while the hydrogen evolved in the left-arm of the U-tube was trapped over the falling level of the solution, below the stop-cock 'f'. When the level of the solution approached the electrode at the bottom, the electric current was stopped and by opening the stop-cock 'f' the amount of generated hydrogen was admitted into the already evacuated and out-gassed calcium chloride trap. After raising the level of the solution in left-arm upto the stop-cock 'f', by raising the reservoir, both the stop-cocks 'e' and 'f' were closed and the operation of electrolysis was repeated.

In this manner, hydrogen could be generated and stored in the calcium chloride trap at a sufficient pressure. The pressure of the generated hydrogen, noted by the Vacustat in the preliminary trials, was related to the number of times the quantity of hydrogen occupying the volume of the left-arm of the U-tube was admitted into the calcium chloride trap. In the final measurements, when the Vacustat was substituted by a blind glass-cone to eliminate the mercury vapour contamination, the pressure of the available hydrogen

in the calcium chloride trap could be estimated from the count of the storing operations.

3.2.5 Since the generated hydrogen was initially collected over the solution, it contained much water vapour. It was, therefore, stored in the calcium chloride trap, usually overnight, with the three stop-cocks 'a', 'b' and 'e' closed. On the following morning, when it was admitted beyond the stop-cock 'a', it again passed through a fresh phosphorus pentoxide trap before entering the discharge tube via stop-cock 'd'. The pressure of the gas (either air or hydrogen) inside the discharge tube was measured with the oil-manometer with an accuracy of about 0.05 mm. of mercury (see 3.2.1.).

3.2.6 The results for hydrogen, as described in chapt. IV, were first obtained on this set-up, with hydrogen handled in this way. However, in measurements with higher pressures and currents, the discharge conditions were often unstable with indications of impurity, the water vapour being the principle suspect. Later the vacuum system B, which is shown in Fig. 6, became available, with which improved conditions of purity could be obtained. The hydrogen measurements were subsequently repeated on that system. The general results in both cases were identical and in a few cases where the purity stage of hydrogen could have any influence, the

observed variations are indicated in the results.

3.2.7 The entire measurements for air, described in chapt. IV, were obtained by using the vacuum system A (Fig. 5). In this case, the U-tube and the reservoir of the electrolysis apparatus were empty, and air was admitted into the system via stop-cock 'f'. As in the case of hydrogen, the air was also stored, first over calcium chloride, overnight, to remove water vapour and was later passed over fresh phosphorus pentoxide, before admission to the discharge tube. Thus the measurements represent the results in the case of dry air. The Vacustat was only used in the initial stages to measure the degree of evacuation and was removed from the system during actual measurements, in order to avoid contamination by mercury vapour.

3.3 VACUUM SYSTEM B: This second system, with which the experiments with hydrogen were subsequently performed under conditions of better purity, is shown schematically in Fig. 6. [Kaufman (1954)]. The general features of this system, which was also made of Pyrex glass, were similar to those of system A, shown in Fig. 5. The main distinguishing feature of the system B was the provision of a vapour pump in series with the rotary backing pump. The horizontal manifold of this system was connected at one end to the vacuum pumps and carried an oil-manometer at the other end, as shown in Fig. 6. The discharge tube was joined to the manifold near the

stop-cock 'F' via a stop-cock 'G', which could isolate the discharge tube from the entire system.

3.3.1 Backing Pump: The rotary vacuum pump used for backing the vapour pump on this system was an "Edwards Speedivac† " type 1 SP 30, with an ultimate vacuum of 0.002 mm. of mercury. It was mounted on anti-vibration mountings fixed to the floor beside the trolley on which the rest of the vacuum system was assembled. A phosphorus pentoxide trap was provided in between this pump and the vapour pump.

3.3.2 Vapour Pump: This was a "Metrovac‡ " single stage oil-diffusion pump, in which "Silicone oil DC703§ " was used as a fluid, giving an ultimate vacuum of 10^{-6} mm. of mercury. The pumping speed was estimated to be about 7 litres per second. In view of the small volume of the system and consequent short time of pumping, the silicone oil could be safely used without any cold trap. The vapour pump was water cooled during its operation. An half inch "Edwards‖ vacuum union", modified as described later in 3·3·4, was hard soldered to the top flange of the vapour pump and this mated with the vertical glass tube attached to the bottom of the socket of the stop-cock 'F'.

---

† W. Edwards and Co. (London) Ltd.
‡ Metropolitan Vickers Co. Ltd. (Manchester, England)
§ Dow Corning Corporation (Michigan, U.S.A.). Sole Distributors: W. Edwards and Co. (London) Ltd.
‖ W. Edwards and Co. (London) Ltd.

3.3.3 The oil-manometer: Unlike the oil-manometer on the system A, which had only one spherical bulb protecting both limbs and a single stop-cock to isolate only one limb, the manometer on this system had a separate spherical bulb protecting each limb and had two stop-cocks 'D' and 'E' which enabled the isolation of both of the limbs from the manifold, if necessary. This was particularly useful in reducing the desorption of the glass limbs, which was proportional to the total time for which the manometer limbs were evacuated. Thus all the pumping hours during preliminary trial experiments could be added up, since the complete manometer could be isolated by closing the stop-cock 'E', whenever the manifold was opened to the atmosphere. It was estimated that when the final observations were made, the manometer had been subjected to about 250 hours of pumping with the vapour pump. With such a prolonged pumping, together with periodic treatments for out-gassing by the 20 kc/s-frequency-discharge from a "Tesvac", removed all the adsorbed gases from the manometer, although it could not be baked, as the rest of the system, with an electrical heating tape.

The fluid used in the manometer was also DC 703 with a magnification ratio of 12.45 at 20°C with respect to mercury. The scale made for this manometer was, therefore, engraved in such a manner that

249 millimeters of its length were divided into 400 equal divisions, each corresponding to 0.1 mm. of mercury. Since the maximum difference in the bore of the two limbs of this manometer was found to be about 3.5 per cent - as against one per cent in the case of the manometer on system A - the manometer was used differentially by noting the difference between the oil levels in both the limbs in number of engraved divisions, and dividing it by 2 to obtain the pressure reading in tenths of millimeters of mercury. The scale of this manometer was silvered at the back for anti-parallax purposes and using a magnifying glass of about 60 mm. focal length to read the oil levels, the pressure measurements could be made with an accuracy of 0.05 mm. of mercury. The manometer was found quite sensitive in indicating the difference between the degrees of ultimate vacuum obtained with only the rotary pump and that obtained with the rotary and vapour pump operating together.

3.3.4 The Gas Supply System: Since this system had provisions to obtain better conditions of purity, a supply of spectroscopically pure hydrogen was used to obtain the desired gas pressure in the discharge tube. A litre of 99.998% pure hydrogen was obtained in a Pyrex glass vessel from the British Oxygen Co. Ltd., and according to the data

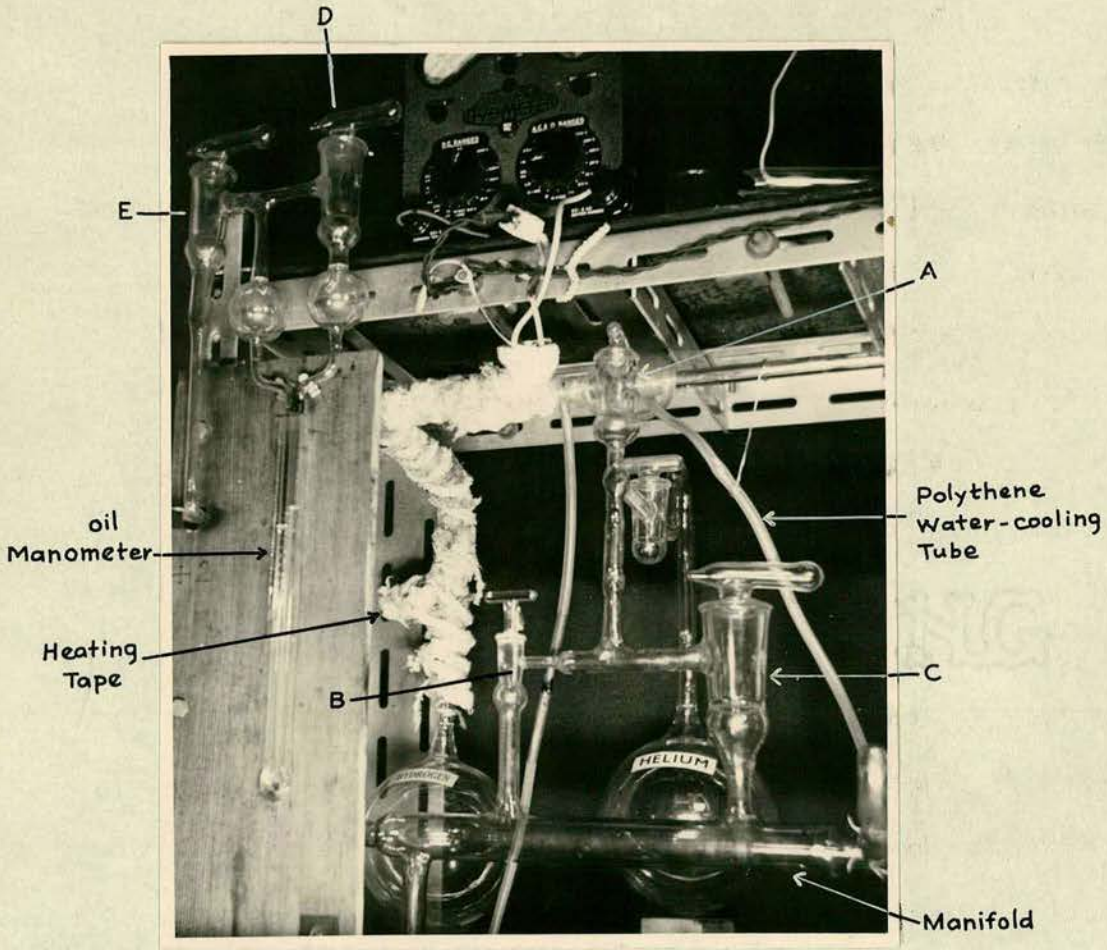
D
E
A
Polythene
Water-cooling
Tube
oil
Manometer
Heating
Tape
B
C
HELIUM
Manifold

FIG. 7.

supplied by the manufacturers the purity of the gas was estimated as follows:

Hydrogen	999980	v.p.m.†
Nitrogen	12	v.p.m.
Oxygen	3	v.p.m.
Carbon Monoxide ...	3	v.p.m.
Carbon dioxide ...	2	v.p.m.

The vertical neck of this gas-bottle was provided with a special seal-breaking device as described in detail in Appendix B. The neck of the gas-bottle was then joined, via the stop-cock 'A', to another short manifold having two more stop-cocks 'B' and 'C' at its ends, which opened into the main manifold. Before breaking the seal of the gas bottle, its neck, together with the entire seal breaking device, as well as the short manifold between the stop-cocks 'B' and 'C' was thoroughly evacuated with the vapour pump over a long period and at the same time the glass was baked using the heating tape. In Fig. 7 is shown a photograph of this part of the vacuum system, taken during the baking operation. The stop-cocks were protected from excessive heat by coiling a polythene tube around them (as shown in the photograph), through which cold water was circulated.

Out of the two stop-cocks 'B' and 'C', 'B' was of a large bore, permitting the fast pumping of the neck of the gas-bottle and of the short manifold BC. After evacuation and thorough out-gassing, the stop-

---

† The abbreviation v.p.m. represents unit volume per million unit volumes, i.e., 1 v.p.m. = 0.0001%.

cock 'C' was closed and remained closed thereafter. Before breaking the seal of the gas bottle, the stop-cocks 'A' and 'B' were also closed, and after breaking the seal, the gas was first admitted to the short manifold BC by opening the stop-cock 'A' and then further into the main manifold via stop-cock 'B', which had a solid key with an L-shaped fine capillary bore for slow leaking.

3.3.5 Desorption of Glass: All the parts of the vacuum system, which were made of Pyrex glass, were desorbed by heating with an "Electro-thermal† " heating tape type 201, except the stop-cocks and the oil-manometer which was out-gassed by a "Tesvac" as described earlier in 3.3.3. Different sections of the system were wrapped, part by part, with the heating tape, over which two layers of fibre glass were lagged to reduce radiation losses. Measurements with an iron-constantan thermocouple, placed in contact with the glass below the heating tape, indicated that for glass tubes between 10 and 30 mm in diameter, a baking temperature of about 300°C can be obtained after 15 to 20 minutes. During the baking operation, the greased stop-cocks were protected from excessive heat by a water cooling system using a polythene tube as shown in Fig. 7. All the stop-cocks were greased with "Apiezon" grease L, having a vapour pressure of 10^{-10} mm. of mercury at room temperature.

---

†Electro Thermal Engineering (London) Ltd.

FIG. 8.

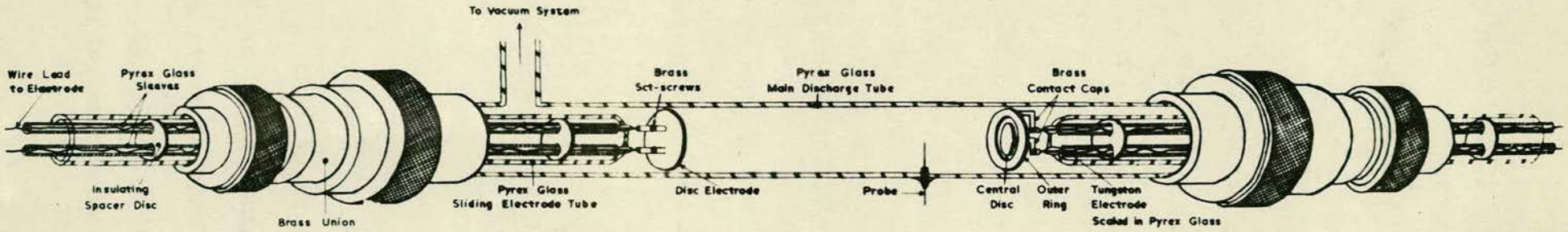
To Vacuum System
Wire Lead to Electrode
Pyrex Glass Sleeves
Brass Set-screws
Pyrex Glass Main Discharge Tube
Brass Contact Caps
Insulating Spacer Disc
Brass Union
Pyrex Glass Sliding Electrode Tube
Disc Electrode
Probe
Central Disc
Outer Ring
Tungsten Electrode Sealed in Pyrex Glass

3.4 THE DISCHARGE TUBE: The discharge tube, used for measurements with both hydrogen and air, is shown schematically in Fig. 8. It was desired to make the probe measurements in different regions of the glow discharge, and for this purpose a fixed probe was used, with respect to which the discharge column of the gas was moved by changing the position of the two electrodes placed on either side of the probe.

3.4.1 The Main Discharge Section: The central section between the two brass couplings (see Fig. 8), which was 417 mm. in length, constituted the main vessel, in which the glow discharge was confined. It was made of Pyrex glass tube with a circular cross-section of an inside diameter of 20 mm. The thickness of the wall was about 1.0 mm. At a distance of 45 mm. from one end, a T-joint was made, forming an exhaust, at which the tube was joined to the main manifold via the stop-cocks 'd' and 'G' of the two vacuum systems A and B respectively. (see Figs. 5 and 6).

3.4.2 The Probe: Theprobe was sealed into the wall of the main discharge section, at a distance of 230 mm. from the exhaust tube, as shown in Fig. 8. It was made from a tungsten wire, 0.2 mm. in diameter. In order to make a good vacuum seal in Pyrex glass, it is necessary to remove the oxide coating from

the surface of the tungsten. Such a cleaning of the probe wire surface was effected by electrolysis in a 20% solution of sodium hydroxide. [Partridge (1949) p. 36.] A copper plate was used as the cathode, a short distance in front of a loop of tungsten wire serving as the anode. It was found from trials that best cleaning could be achieved by passing a strong direct current of about 4 amperes through the solution for a short time of about 80 seconds.

Before making a seal, the metal has also to be outgassed. The normal method of heating in a flame could not be used because of the very fine diameter of the wire. The outgassing was therefore done by placing short pieces of the cleaned tungsten wire in a silica glass tube, which was heated red hot by two Bunsen burners for one hour. During the heating, the silica tube was joined to the vacuum system and was continuously evacuated in order to prevent oxidation of the cleaned surface and also to induce the desorption of the metal.

After the pieces of the tungsten wire were cooled in vacuum to the room temperature, they were taken, one by one, out of the silica tube and were immediately sealed in beads of C9 glass, near one of their ends. These seals were later annealed in an electrical oven over a period of eight hours. A scrutiny of the finished seals under a microscope, revealed that two seals out of five had been obtained which were free

from any gas bubbles around the portions of the wires in the glass beads and which exhibited the characteristic golden-brown colour of a good tungsten seal. One of these pieces was used as a probe. Because of the electrolytic cleaning, the diameter of the tungsten wire was reduced from its nominal value of 0.2 mm. and the actual diameter of the finished probe was measured under a travelling microscope as 0.12 mm. The short end of the wire beyond the glass bead was also cut under the microscope, leaving a length of the exposed part of the probe exactly equal to 5 mm. A small hole was made in the wall of the Pyrex glass discharge tube, and the probe was assembled in place by fusing the C9 glass bead to Pyrex. When in position, the probe wire was radial to the circular cross-section of the discharge tube, with its tip at the centre.

3.4.3 The Electrodes: The glow-discharge in the tube was obtained using two circular plane electrodes on either side of the probe. In all the earlier experiments for the study of the light effect on a.c. discharges (as summarised in 1.5), the role played by the walls of the discharge vessel in influencing the mechanism of the discharge had been stressed. A special geometry was, therefore, used for the electrodes in the present study. Out of the two disc electrodes made from an aluminium sheet of 1/16 inch thickness, the one nearer the probe, which was used

as the anode, was split concentrically into a central disc and an outer annular ring (see Fig. 8). Individual leads were provided to the two sections of the electrode; consequently, the part of the total current carried by each of them could be studied separately for the effects of external visible light. The two sections of the electrode were turned out on a precision lathe, exactly to the following dimensions:

CENTRAL DISC: Outer Diameter 10.0 mm.

OUTER RING: Outer Diameter 19.5 mm.

Inner Diameter 13.4 mm.

These dimensions were chosen so that the annular separation between the disc and the ring was of a reasonable width of 1.7 mm. and at the same time a round figure of 2 was obtained for the ratio of the area of the outer ring to the area of the central disc.

The other electrode, used as the cathode, was a disc, in one piece, of a diameter of 19.5 mm, which was equal to the outside diameter of the ring of the anode. It was also cut off a sheet of aluminium, 1/16 inch thickness. Small brass contact-caps were attached to the back of the cathode as well as of the two sections of the anode as shown in Fig. 8. (Page 40). The other ends of these contact-caps were bored to fit over the projecting ends of two pairs of short tungsten rods, about a millimeter in diameter. These two pairs of tungsten rods were sealed, one each, in the ends of two Pyrex glass hollow tubes, such that they

protruded about 7 mm. on either side of the seal. These Pyrex tubes, which are marked as "Pyrex glass sliding electrode tubes", in Fig. 8, were 17 mm. in diameter, 300 mm. in length and had wall thickness of about 1.5 mm. At one end, the sealed tungsten rods carried the brass-contact-caps, which were secured by tiny grub screws; and their other ends were spot welded to long pieces of braided copper wires, running along the inside of the Pyrex tubes. These two copper wires served as electrical leads via the brass contact-caps, jointly to the cathode through one sliding electrode tube† and separately to the two sections of the anode through the other. These leads were electrically insulated from each other by Pyrex glass sleeves over their entire lengths. The movement of the sleeves inside the sliding electrode tubes, which could cause a strain on the tungsten rod seals, was prevented by putting them through spacer-discs (see Fig. 8). These spacer-discs, which were a tight fit inside the sliding electrode tubes, were turned out of a 1/16 inch thick sheet of "Paxolin".

3.4.4 The Couplings: The two sliding electrode tubes carrying the anode and the cathode were held in the main discharge tube by two brass couplings,

---

† The purpose of providing two leads also through the other tube, which carried the single-piece electrode, was to enable the same electrode tube to be used for carrying a filament. The results in the case of hot-cathode discharges are, however, not embodied in the present thesis.

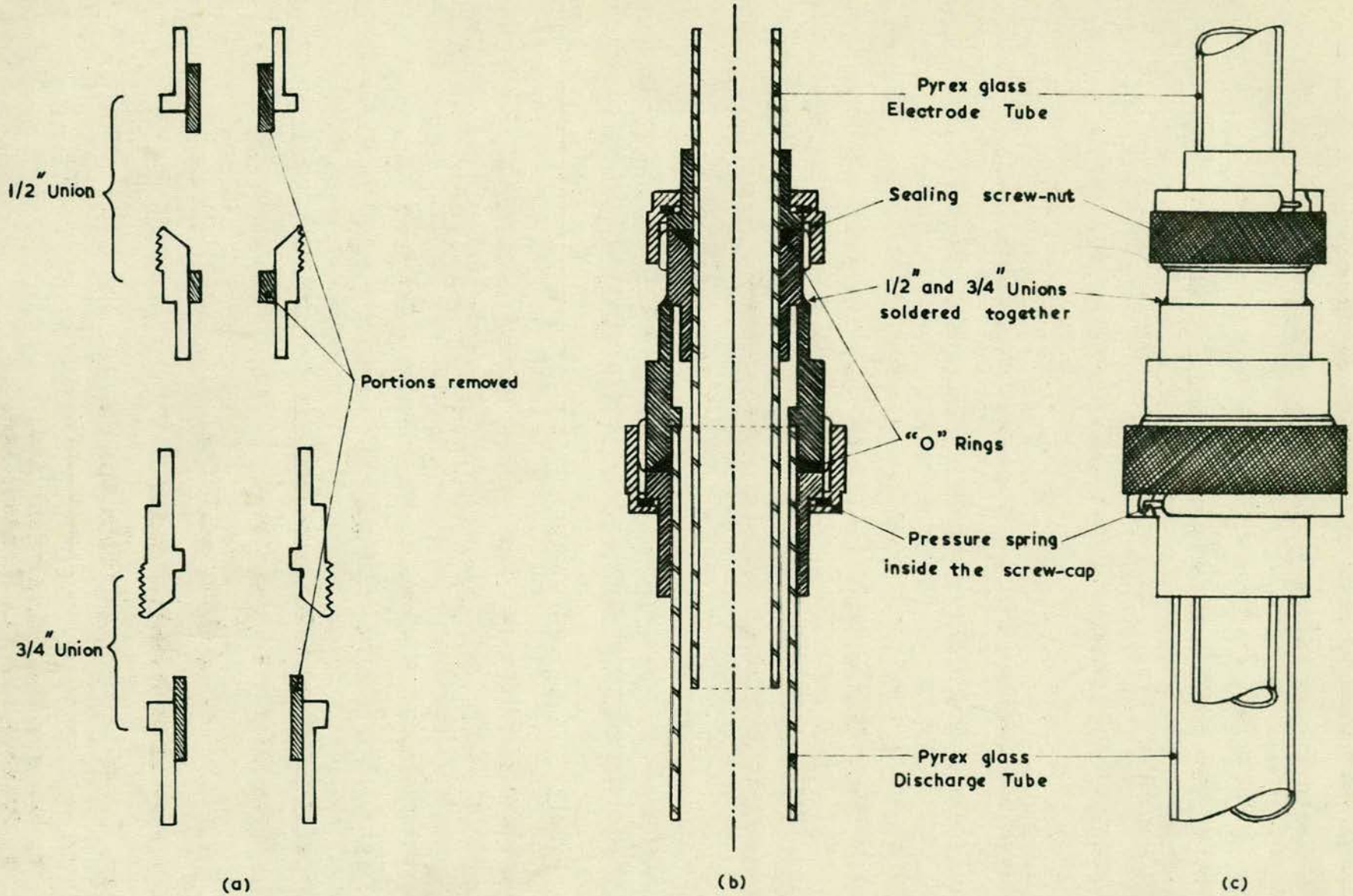
1/2" Union
Portions removed
3/4" Union
Pyrex glass
Electrode Tube
Sealing screw-nut
1/2" and 3/4" Unions
soldered together
"O" Rings
Pressure spring
inside the screw-cap
Pyrex glass
Discharge Tube
(a)
(b)
(c)

FIG. 9.

which maintained a vacuum-tight joint. Each of these couplings was made by modifying a pair of "Edwards† ½ inch and 3/4 inch standard unions" as shown in detail in Fig. 9. In Fig. 9(a) is shown a sectional drawing of the parts of the standard unions, without the knurled locking nuts. Three out of these four parts were modified by turning them on a lathe to remove some of their portions as indicated in the drawing (a). The modified parts of the 3/4 inch and ½ inch unions were required to have a close sliding fit over the main discharge section and the sliding electrode tube respectively. The middle two parts were then soldered together and the modified unions were assembled as shown in section in Fig. 9(b). The vacuum seal was maintained by two "elastomer‡ 'O' rings" one stretched over the outside of the main discharge tube and the other over the outside of the sliding electrode tube. The original circular cross-section of these rings was squeezed into a triangular shape, by the locking nut, to press against parts of the brass unions on two sides and against the glass on the third. The locking nuts only needed a hand tightening. The 'O' rings were used dry and with all the surfaces scrupulously cleaned free from grease and dirt, a perfect vacuum seal could be consistently obtained. Fig. 9(c) shows the outside view of an assembled unit.

With these couplings, both the cathode and the

---

† W. Edwards and Co.(London) Ltd.
‡ W. Edwards and Co. (London) Ltd.

anode could be easily moved inside the main discharge tube as required. It was also found that by slackening the locking nut on the $\frac{1}{8}$ inch union by half a turn, the sliding electrode could be pulled in slowly, by virtue of the difference of pressure between the outside and the inside of the discharge section. The rate of this movement could be controlled by adjusting the slack on the locking nut. Movements as slow as a couple of millimeters within one hour were often possible. During the movements at such a slow rate, there was no indication of a loss of vacuum on the oil-manometers, whose sensitivities were 0.05 mm. of mercury as given earlier in 3.2.1 and 3.3.2. Such a movement of the electrodes was particularly useful in making fine adjustments of the inter-electrode distances to any exact value and also to avoid the hollow cathode effects on the discharge currents [Little (1953)], arising from a slight sputtering of the electrodes. Usually the separation between the cathode and anode was kept initially more than the desired value and having run the discharge for some time, after there was no more sputtering, both the electrodes could be slightly pulled in to occupy new positions surrounded by clean glass-walls. The desired separation was exactly obtained by controlling the movement as mentioned earlier.

3.5 ELECTRICAL EQUIPMENT: For the experiments

with air, done on vacuum system A (Fig. 5), the high tension d.c. supply was obtained from a 4kV voltage doubler circuit, ~~which is shown schematically on the left hand side of Fig. 13.~~ A "Cintel†" stabilised power pack Type 1892 was used for the high tension d.c. supply for experiments with hydrogen, conducted on the vacuum system B (Fig. 6). The applied voltage was measured by two electrostatic voltmeters having ranges 300-50-1500 volts and 500-100-3000 volts. Details of other auxiliary circuits for electrical measurements are given in Chapter IV separately in each case.

3.6 SOURCE OF VISIBLE LIGHT FOR EXTERNAL IRRADIATION: For the study of the effect of external visible light, the discharge tube was irradiated with white light from three "Ediswan‡" incandescent lamps rated at 100 watts each. These lamps, which had frosted glass bulbs, were mounted in a row inside a wooden box 3.5" x 6.5" x 18". The entire interior of the wooden box was covered with 1/16 inch white asbestos sheets, as a protection against excessive heat. A few 1/4 inch holes were also made in each face of the box for ventilation. The distance between the centres of two adjoining lamps was 120 mm. The discharge tube was irradiated by placing the lamp box beside it, with the line of the centres of the lamps parallel to the tube.

---

†Cinema Television (London) Ltd.
‡Edison Swan and Co. (London) Ltd.

3.6.1 Earlier workers, working with a.c. discharges, have reported a logarithmic relation (see 1.5.5) between the effect on the current and the intensity of the light, as shown in Fig. 1(E). In the present study with d.c. discharges, the % effect of light (see footnote on page 14) on the current was very small and measurements of the relative changes with the variation of the intensity of the source over a limited range (possible by varying the distance of the lamp-box from the discharge tube) were difficult to be made with sufficient accuracy. Due to lack of space, large variations in the distance of the lamp-box from the discharge tube were not possible. A method of controlling the intensity by using polaroids was tried as an alternative. However, it was found to introduce complications, as described in detail later in 4·3·8 , which were unfortunately inherent.

No attempt was, therefore, made in the present study to vary the intensity of the irradiating source. All measurements were made with the line of the centres of the lamps 120 mm. away from the discharge tube. The intensity of the light falling on the discharge tube was estimated by using a photo-electric cell, which was calibrated against a 60 watt incandescent lamp, used as a subsidiary standard by virtue of a certificate of its performance from the Photometric Laboratory of Everett Edgcumbe and Co. (London) Ltd. The calculated value of the intensity

falling on the discharge tube was 11·27 lumens per cm^2, and was found to be fairly constant over the entire length of the discharge tube. The continuous emission spectrum of one of the incandescent lamps is shown in Fig. 17 .

CHAPTER IV.

EXPERIMENTAL RESULTS.

Section I: Measurements with a Probe.

4.1.1 As mentioned earlier in 1.5, the effect of visible light on low pressure discharges had been previously studied extensively in the case of a.c. discharges. However, a survey of the available literature on the subject at once reveals that although it had been studied for different conditions of the auxiliary parameters like the type of gas, its pressure, the frequency and the intensity of irradiating light etc. the only measurements made were those of the discharge current. Since the discharges were excited with alternating potentials, various types of detectors had indeed been used, and sometimes a search had also been made to detect frequencies other than that of the applied potential. These changes of instrumentation, however, did not, in any way, influence the relation of the measured parameter (which had been essentially the discharge current, i) to the fundamental processes of the discharge, which themselves are complicated for alternating potentials.

4.1.2 The main attention of this study was directed towards making direct measurements of the concentrations of charged particles. As discussed earlier in 1.10, a possibility of an increase in the

average mass of the charged particles could be inferred as a consequence of the observed reduction in the average mobility of the charged particles. A mass-spectrographic study should be helpful for such an analysis. The influencing factor is the inherent resolving power of the instrument, since the mobility is inversely proportional to the square root of the mass (see equation 1.10.1). The use of a conventional magnetic mass-spectrometer is further limited by the bulkiness of the apparatus; and because of the inevitable long path length of ions in the analyser of such an instrument, the difficulties of screening the discharge tube from the magnetic field make it impossible to obtain the required sensitivity. For studying the effect of light, it would also be imperative, for irradiation, to keep the discharge tube out of any shielding.

The technique of a radio-frequency mass spectrometer probe, recently developed by Boyd (1950b), appeared promising from this point of view, but could not be adapted to the present study because of the limitations of the available facilities. An ordinary Langmuir probe, as described earlier in 3.4.2, was, therefore, used in these investigations.

4.1.3 The Theory of Using a Probe: By studying the current-voltage characteristic of a small probe inserted in a gas discharge, Langmuir & Mott-Smith (1923) and later Langmuir (1925) developed a theory

FIG. 10.

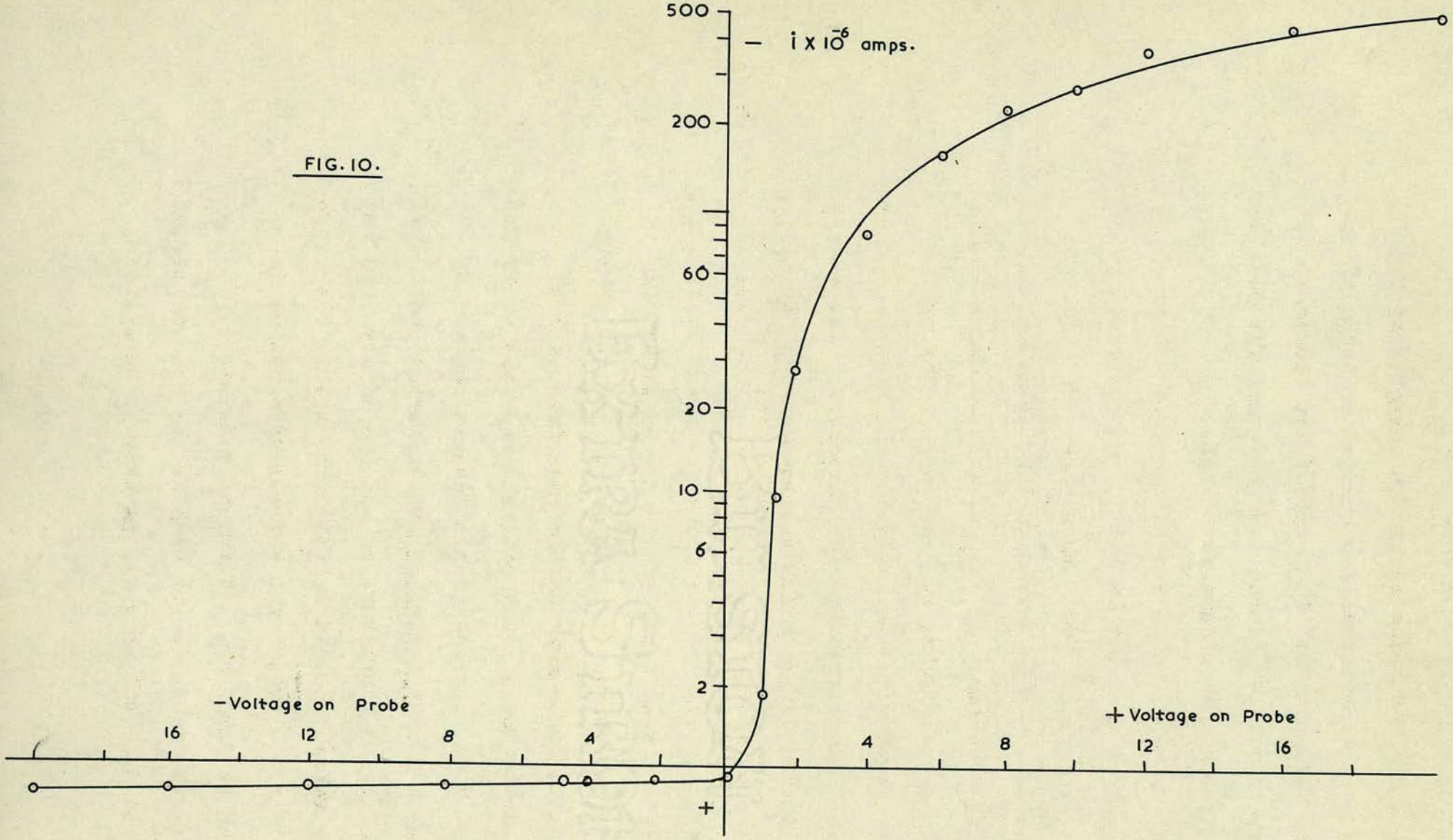
500
200
60
20
10
6
2
− i X 10⁻⁶ amps.
−Voltage on Probe
16
12
8
4
+
+ Voltage on Probe
4
8
12
16

to derive the knowledge about the energies of the charged particles (usually expressed in terms of the electron "temperature" T_e , and/or ion "temperature" T_i), the densities of the electrons and the positive ions and about the plasma potential.

4.1.3(a) A detailed discussion of the limitations in the use of a simple Langmuir probe is given by Loeb (1947, pp. 251-256), which need not be quoted here again. The primary requisite of having the effective resistance of the probe large compared to the medium surrounding it, was achieved by making the measurements in the plasma of the discharge, where high ionic concentrations are expected. The validity of the assumption of a Maxwellian distribution for energies, is indicated by the linearity of the slope of the obtained semilogarithmic V-i characteristic of the probe, as shown in Fig. 10.

4.1.3(b) When using probes for investigating inside a discharge, the pressure of the gas should have a value such that the mean free path of electrons is large compared with the diameter of the probe. From the experimental determinations by Townsend & Tizard (1913) of the electronic mean free path in air at a pressure of 1.0 mm. of mercury, the minimum value obtained is 0.271 mm. within the range of $0.5 < X/p < 100$. The corresponding value for hydrogen is 0.205 mm. [Townsend & Bailey (1921)] . The diameter of the probe used in the present study which was 0.12 mm. as given earlier in 3.4.2, was,

thus, less than the minimum possible values for the electronic mean free path in both air and hydrogen.

4.1.4 As discussed earlier in 1.9, it appeared that the reduction in the discharge current, on exposure to visible light was probably due to a reduction in the number of charged particles. Further, this loss was thought to be mainly due to the attachment of electrons to form negation ions. (see 1.9.6).

4.1.5 When a probe is at large negative potentials with respect to the surrounding gas, it receives only the positive ions, but at higher potentials (algebraically) it begins to collect progressively more and more electrons and also negative ions, according to their velocities. Hence the current drawn by the probe, when it is above the "floating potential", is a compound measure of the contributions by the electrons and negative ions. It is, therefore, not possible to get any individual information about the amount of loss in the total number of electrons, and about the number of negative ions present, unless the probe is equipped with an auxiliary grid [Boyd (1950a)], which may effect a selection of ions by virtue of their higher masses and consequent lower velocities. Attempt was, therefore, only made in the present study, to measure the saturation positive-ion current to the probe. The probe was

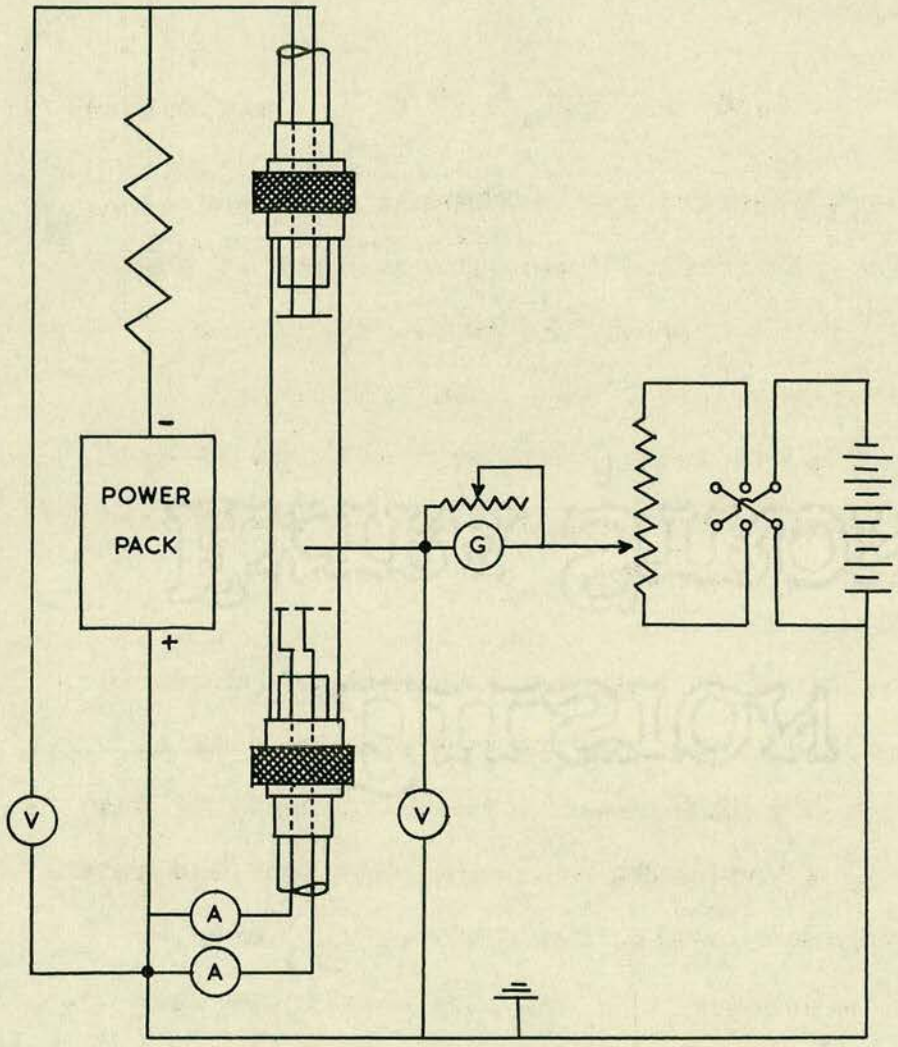

FIG. 11.

exposed to the central half of the discharge column (see 3.4.2). Since the curves, as shown in Fig. 10, indicated a marked saturation of the positive-ion current, the positive-ion densities could be calculated [Guthrie & Wakerling (1949, p. 14)] by means of the expression

$$i_+ = 0.40 \stackrel{?}{e} N_+ (2KT_e/M_+)^{\frac{1}{2}} A \qquad \ldots(4.5.1.)$$

where i_+ is the positive-ion current in ions per sec., N_+ the density of positive ions, M_+ the mass of the positive ion, A the area of the probe, T_e is the electron temperature and K Boltzmann's constant. The quantity KT_e was evaluated from the slope of the linear function of the potential of the probe to the logarithm of the current flowing to the probe.

4.1.6 The probe current was measured, as shown in Fig. 11, by a Cambridge† spot galvanometer having a sensitivity of 6×10^{-9} amperes per deflection of one mm. By using a hand-made paper vernier over the face of the galvanometer scale, the deflections were estimated to a quarter of a mm. A commutator with different fixed resistances was provided for shunting the galvanometer to a series of higher ranges. As shown in Tables I-VIII on the following pages, the saturation positive ion current to the probe was found to diminish on exposure to external visible light.

---

†Cambridge Instrument Co. (England) Ltd.

4.1.7 The positive column of a discharge is known to have a uniform field, and when a large concentration of negative ions is built up, an equal concentration of positive ions at each point is required to maintain the equilibrium. Some times the negative ions set up regions of negative space charge when suitable conditions for formation of striations could be built up. In each case, the probe measurements were, therefore, made once with the probe enveloped with the glow of a striation, and secondly with the probe at the centre of the dark region in between two adjacent striations. These are indicated in tables II to IV and VI to VIII. In the cases of tables I and V, where the pressure was the lowest, stable striations were not obtained.

4.1.8 The measurements with the probe, were corroborated with the measurement of the discharge current in a special manner. As mentioned earlier in 3.4.3, a split-electrode geometry was used, to measure the discharge current in parts. Because of their small mass and hence large random motion, the space distribution of the electrons in a plasma can usually be described by a Boltzmann relation, involving an electron temperature [Tonks & Langmuir (1929b)]. The massive positive ions tend, however, to move unidirectionally along the lines of force, and a very similar behaviour of negative ions could also be reasonably expected. In the positive column the axis

is positive relative to the walls, so the negative ions would tend to concentrate along the axis. As a result, most of the contribution to the discharge current by negative ions could be expected in the part collected by the central disc of the anode, while the part collected by the outer ring would be mostly electronic. The effect of visible light was found confined only to the current collected by the outer-ring which showed a decrease on irradiation, as given in tables I to VIII.

4.1.9 The light effect had been studied in the case of a.c. discharges, under different conditions of six parameters, as mentioned earlier in 1.5.1 to 1.5.6. Out of these, a variation in the frequency of the applied potential was not applicable to the present study in d.c. discharges. For reasons mentioned earlier in 3.6.1, the intensity of the irradiating source was kept constant throughout the present study. It was also not possible to study the effect of different frequencies for irradiation, since the intensity of the filtered light was not sufficient to make accurate measurements. In the case of hydrogen, the observations were not influenced by any "ageing " effect, but in the case of air, slight variations occurred at two higher pressures, which are indicated in tables III and IV. The effects of varying the applied potential and the pressure of the gas were investigated

in the present study.

4.1.10 For each of the two gases, air and hydrogen, the measurements were made at four different pressures, with four different values of applied potential for each pressure. These results are given on the following pages as tables I to IV in the case of air and as tables V to VIII in the case of hydrogen.

TABLE I

Measurement of the saturation current to a Negative Probe, and of the discharge current by a split anode, in a discharge in Air at a pressure p = 1.35 mm. Hg.

ANODE CURRENT ON CENTRAL DISC		ANODE CURRENT ON OUTER RING				SATURATION CURRENT TO A NEGATIVE PROBE (i_+)	
i_D mA	i_L mA	i_D mA	i_L mA	$-\Delta i$ mA	% $(-\Delta i)$	in Dark $\times 10^{-7}$ A	under Light $\times 10^{-7}$ A
0.25	0.25	1.050	1.038	0.012	1.14%	4.65	4.55
0.40	0.40	1.580	1.561	0.019	1.20%	6.85	6.80
0.50	0.50	2.020	1.994	0.026	1.30%	8.80	8.65
0.60	0.60	2.350	2.313	0.037	1.50%	10.2	10.05

$N^+ = i_+$ (in amps) $\times 5.230 \times 10^{17}$ ioms/cm^3.

TABLE II

Measurement of the saturation current to a Negative Probe, and of the discharge current by a split anode, in a discharge in Air at a pressure p = 1.56 mm. Hg.

ANODE CURRENT ON CENTRAL DISC		ANODE CURRENT ON OUTER RING				SATURATION CURRENT TO A NEGATIVE PROBE (i_+)			
						Probe in Striation		Probe in Dark space	
i_D	i_L	i_D	i_L	$-\Delta i$		in Dark	under Light	in Dark	under Light
mA	mA	mA	mA	mA	$\%(-\Delta i)$	$\times 10^{-7}$ A	$\times 10^{-7}$ A	$\times 10^{-7}$ A	$\times 10^{-7}$ A
0.30	0.30	1.190	1.173	0.017	1.42%	5.15	5.09	4.85	4.82
0.40	0.40	1.670	1.643	0.027	1.62%	7.25	7.15	6.93	6.92
0.50	0.50	2.100	2.064	0.036	1.72%	9.10	8.95	8.50	8.50
0.65	0.65	2.510	2.465	0.045	1.80%	10.9	10.4	10.0	9.80

$N^+ = i_+$ (in amps) $\times 5.352 \times 10^{17}$ ions / cm^3.

TABLE III

Measurement of the saturation current to a Neagtive Probe, and of the discharge current by a split anode, in a discharge in Air at a pressure p 1.86 mm. Hg.

ANODE CURRENT ON CENTRAL DISC		ANODE CURRENT ON OUTER RING				SATURATION CURRENT TO A NEGATIVE PROBE (i_+)			
						Probe in Striation		Probe in Dark space	
i_D mA	i_L mA	i_D mA	i_L mA	$-\Delta i$ mA	$\%(-\Delta i)$	in Dark $\times 10^{-7}$ A	under Light $\times 10^{-7}$ A	in Dark $\times 10^{-7}$ A	under Light $\times 10^{-7}$ A
0.35	0.35	1.340	1.320	0.020	1.49%	5.83	5.75	5.47	5.47
						5.61	5.45	--	--
0.45	0.45	1.770	1.738	0.032	1.81%	7.70	7.55	7.21	7.21
						7.61	7.46	7.15	7.15
0.55	0.55	2.170	2.126	0.044	2.03%	9.45	9.23	8.77	8.76
						9.40	9.11	--	--
0.65	0.65	2.560	2.501	0.059	2.30%	11.2	10.9	10.2	10.1
						--	--	--	--

The probe current values in the second line, in each row, were obtained after running the discharge for an hour, indicating the influence of 'ageing' .

$N^+ = i_+$ (in amps) $\times$ $5 \cdot 699 \times 10^{17}$ ions/cm^3.

TABLE IV

Measurement of the saturation current to a Negative Probe, and of the discharge current by a split anode, in a discharge in air at a pressure p 2.12 mm. Hg.

ANODE CURRENT ON CENTRAL DISC		ANODE CURRENT ON OUTER RING				SATURATION CURRENT TO A NEGATIVE PROBE (i_+)			
						Probe in Striation		Probe in Dark space	
i_D mA	i_L mA	i_D mA	i_L mA	$-\Delta i$ mA	% $(-\Delta i)$	in Dark $\times 10^{-7}$ A	under Light $\times 10^{-7}$ A	in Dark $\times 10^{-7}$ A	under Light $\times 10^{-7}$ A
0.40	0.40	1.500	1.473	0.027	1.80%	6.52	6.30	6.12	6.12
						6.22	5.90	6.02	6.01
0.50	0.50	1.900	1.860	0.040	2.10%	8.25	8.10	7.72	7.71
						8.05	7.82	7.64	7.62
0.60	0.60	2.290	2.237	0.053	2.32%	10.0	9.70	9.30	9.30
						9.84	9.50	9.38	9.28
0.70	0.70	2.680	2.612	0.068	2.53%	11.7	11.2	10.6	10.6
						11.5	11.0	10.6	10.6

The probe-current values in the second line, in each row were obtained after running the discharge for an hour, indicating the influence of "ageing".

$N^+ = i_+$ (in amps) $\times$ 5.946×10^{17} ions / cm^3

TABLE V

Measurements of the saturation current to a negative Probe, and of the discharge current by a split anode in a discharge in hydrogen at a pressure p = 1.25 mm. of Hg.

ANODE CURRENT ON CENTRAL DISC.		ANODE CURRENT ON OUTER RING				SATURATION CURRENT TO A NEGATIVE PROBE (i_+)	
i_D mA	i_L mA	i_D mA	i_L mA	$-\Delta i$ mA	$\%(-\Delta i)$	in dark $\times 10^{-7}$ A	under Light $\times 10^{-7}$ A
0.30	0.30	1.250	1.241	0.009	0.74%	22.6	20.7
0.45	0.45	1.820	1.806	0.014	0.77%	30.3	30.1
0.60	0.60	2.350	2.331	0.019	0.81%	39.1	38.8
0.70	0.70	2.800	2.775	0.025	0.89%	46.6	46.3

$N^+ = i_+$ (in amps) $\times$ 9.107 $\times 10^{16}$ ions/cm^3.

TABLE VI

Measurements of the saturation current to a negative probe, and of the discharge current by a split anode in a DISCHARGE IN HYDROGEN at a pressure p = 1.8 mm. of Hg.

ANODE CURRENT ON CENTRAL DISC		ANODE CURRENT ON OUTER RING				SATURATION CURRENT TO A NEGATIVE PROBE (i_+)			
						Probe in Striation		Probe in Dark space	
i_D mA	i_L mA	i_D mA	i_L mA	$-\Delta i$ mA	$\%(-\Delta i)$	in Dark $\times 10^{-7}$ A	under Light $\times 10^{-7}$ A	in Dark $\times 10^{-7}$ A	under Light $\times 10^{-7}$ A
0.40	0.40	1.620	1.605	0.015	0.94%	27.0	26.8	25.5	25.4
0.50	0.50	2.140	2.118	0.022	1.05%	35.5	35.3	33.4	33.4
0.60	0.60	2.570	2.542	0.028	1.09%	42.9	42.4	39.7	39.7
0.75	0.75	3.050	3.013	0.037	1.22%	50.6	50.2	45.6	45.5

$N^+ = i_+$ (in amps) $\times$ 1.045 $\times$ 10^{17} ions / cm^3.

TABLE VII

Measurement of the saturation current to a negative probe, and of the discharge current by a split anode in a discharge in hydrogen at a pressure p = 2.5 mm. of Hg.

ANODE CURRENT ON CENTRAL DISC		ANODE CURRENT ON OUTER RING				SATURATION CURRENT TO A NEGATIVE PROBE (i_+)			
						Probe in Striation		Probe in Dark space	
i_D mA	i_L mA	i_D mA	i_L mA	$-\Delta i$ mA	$\%\ -\Delta i$	in Dark $\times 10^{-7}$ A	under Light $\times 10^{-7}$ A	in Dark $\times 10^{-7}$ A	under Light $\times 10^{-7}$ A
0.45	0.45	1.670	1.654	0.016	0.96%	27.8	27.5	26.0	25.7
0.55	0.55	2.160	2.137	0.023	1.065%	36.0	35.5	33.5	33.1
0.70	0.70	2.640	2.607	0.033	1.25%	44.3	43.6	40.6	40.6
0.80	0.80	3.120	3.076	0.044	1.41%	52.1	51.4	46.5	46.4

$N^+ = i_+$ (in amps) $\times$ 1.157 $\times 10^{17}$ ions/cm^3.

TABLE VIII

Measurement of the saturation current to a negative probe, and of the discharge current by a split anode in a discharge in hydrogen at a pressure p = 2.85 mm. of Hg.

ANODE CURRENT ON CENTRAL DISC		ANODE CURRENT ON OUTER RING				SATURATION CURRENT TO A NEGATIVE PROBE (i_+)			
						Probe in Striation		Probe in Dark space	
i_D mA	i_L mA	i_D mA	i_L mA	$-\Delta i$ mA	$\%(-\Delta i)$	in Dark $\times 10^{-7}$ A	under Light $\times 10^{-7}$ A	in Dark $\times 10^{-7}$ A	under Light $\times 10^{-7}$ A
0.50	0.50	1.800	1.782	0.018	1.00%	30.0	29.7	28.0	28.0
0.60	0.60	2.280	2.253	0.027	1.18%	38.2	37.8	35.5	35.4
						42.6	40.8	40.6	40.5
0.70	0.70	2.760	2.722	0.038	1.38%	45.9	45.3	42.0	42.0
						51.5	50.9	48.1	48.0
0.85	0.85	3.240	3.118	0.052	1.60%	54.2	53.1	48.4	48.4
						61.2	59.4	--	--

The probe current values, in the second line, in the last three rows were obtained in experiments with hydrogen on vacuum system A, and which differed from rest of values obtained on vacuum system B, under better conditions of purity. SEE 3.2.6.

$N_+ = i_+$ (in amps) $\times 1.176 \times 10^{17}$ ions / cm^3.

SECTION II: MEASUREMENTS OF THE NOISE.

4.2.1 It has been known for years that glow discharges, with both hot and cold cathodes and also excited by either a steady potential or an alternating potential, spontaneously generate high frequency oscillations. Appleton & West (1923) were the first to study the ionic oscillations in striated glow discharges, which they found with both hot and cold cathodes. The observed frequencies which were proportional to the anode voltage and to the pressure, within a range of 0.005 to 0.25 mm. of mercury, had values between 1 to 100 kc/s. The observations of Eckart & Compton (1924) in the case of hot cathode arcs are believed to be of brief surges rather than of oscillations. Newman (1924) studied the oscillations of the relaxation type.

Pardue & Webb (1928) found oscillations at frequencies between 20 to 150 kc/s in hot cathode glow discharges, which were independent of the external circuit constants. The values decreased as the gas pressure increased from 0.03 to 0.09 mm. of mercury, and they increased with the anode voltage. These are thought to be plasma-ion oscillations of Tonks & Langmuir.

Tonks & Langmuir (1929a) developed a theory of the oscillations in ionized gases, to account for their observations of H/F oscillations of the order of 1000 Mc/s.

These they termed as plasma electronic oscillations, as against those having lower frequencies of a few hundreds of kc/s, which are called plasma ionic oscillations.

Kniepkamp (1936) has reported oscillations of still lower frequencies - below 1.5 kc/s - for pressures between 0.5 to 5 mm. of mercury. These again were found not due to relaxation but were characteristic of the discharge.

Besides these distinct oscillations, the gas discharge tubes also generate a random noise, which is often present together with the distinct frequencies.

4.2.2 The expression relating the frequency with the concentrations of charged particles, as given by Tonks & Langmuir (1929[a] p. 197) is

$$\nu_e^2 = ne^2/\pi m \quad \text{in the case of electrons} \qquad \ldots.(4.2.1)$$

$$\nu_i^2 = Ne^2/\pi M \quad \text{in the case of ions.} \qquad \ldots.(4.2.2)$$

N and n are the densities of ions and electrons, M and m their respective masses and ν_i and ν_e the frequencies of the plasma-ionic and the plasma-electronic oscillations.

Substituting values of e, m and M for electrons, hydrogen and air ions, in equations 4.2.1 and 4.2.2, we get

$$\nu \text{ electron} = 8980\, n^{\frac{1}{2}} \qquad \ldots.(4.2.3)$$

$$(\nu_i)_H = 200\, N_H^{1/2} \qquad \ldots.(4.2.4)$$

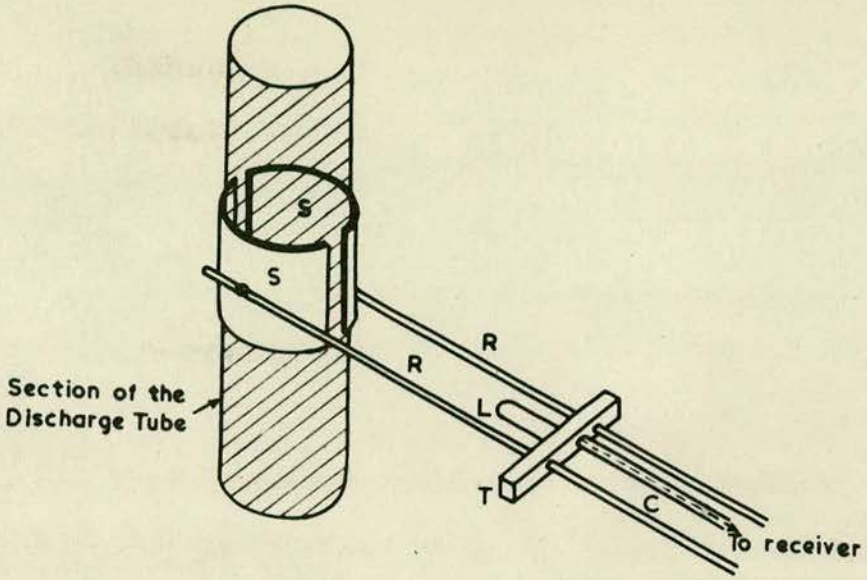

FIG. 12.

$$(\nu_i)_{H_2} = 147.8\ N_{H_2}^{1/2} \qquad \ldots.(4.2.5)$$

$$(\nu_i)_{air} = 38.9\ N_{air}^{1/2} \qquad \ldots.(4.2.6)$$

It is, thus, seen that from the measurement of the frequency of oscillations, a knowledge of the densities of the charged particles could be obtained. Attempt was, therefore, made in the present study to detect the H/F oscillations that may be given out by the discharge, while making probe measurements as described earlier in 4.1.6 and 4.1.7.

4.2.3 The search for the H/F oscillations was made within a range of 20-1000 Mc/s with an intention of noting any changes with the external irradiation which could be checked with the observed reduction of the electronic part of the discharged current, collected by the outer-ring of the split anode, as mentioned earlier in 4.1.9.

4.2.4 Detection of signals: The signals emitted by the discharge were fed to the receiver by a method of external coupling as shown in Fig. 12. The discharge tube was held transversely between two hemi-cylindrical pieces 'S' and 'S', made of copper. These were attached to the ends of a pair of hollow copper tubes 'R' and 'R', having an outer diameter, d, of 6.35 mm. and separated by a distance, s, equal to 33.5 mm. These two formed a parallel-conductor transmission line, which could be tuned to the receiver

by moving the short-circuiting bar 'T'. This bar carried a coupling loop 'L', the output from which was taken to the receiver via a co-axial line 'C'. The size of the loop was not critical and was fixed after a preliminary adjustment. This type of coupling had the advantage that any part of the discharge tube could be placed in between the coupling electrodes, in order to measure the output from different points on the axis of the discharge tube.

Two receivers were used to measure the frequency of the signals. One (type TN-3A/APR-1) was from an ex-U.S. Navy equipment and had a range of 300-1000 Mc/s. The other was a product of the British Admiralty (Type R 1334/10D/779) and its ranges of frequencies were between 20-260 Mc/s, with two gaps between 90-95 Mc/s and 125-135 Mc/s.

4.2.5 These two receivers were calibrated by Marconi standard signal generators. With the help of the internal thermistor bridge on the signal generator, the minimum detectable signal was found to be of the order of 10^{-10} watt, per c/s of band width of about 1 Mc/s. This power, distributed uniformly over the bandwidth, would be equal to that received from a resistance at 6500^{o} K.

The mean electron energy in the discharge was expected to be equivalent to a temperature many times this value, indicating that a large mismatch occurred

between the coupling and the discharge column. The intensity of the oscillations in the discharge was, therefore, always greater by an unknown factor than that available at the receiver input. This belief was substantiated by the fact that when the probe in the tube was used for a direct coupling, the signal at the input of the receiver was much stronger than when using the external coupling. Although the signal strength was higher for a direct coupling, the background noise was also found to be too strong. The external coupling, on the other hand, had the advantage of some tuning and it was also easier to locate it exactly at the particular point where the receiver was found to be most sensitive to the changes. Moreover, since the probe was used for measurements in the positive column at the same time, the external coupling was used for studying the oscillations. Another interesting point was observed in using the probe for a coupling. This probe was situated almost entirely in the central part of the current beam (see 3.4.2), and in spite of a large signal, very little influence of external light could be detected on the oscillations. On the other hand, a tube, wherein the probe was at a very short distance from the wall of the tube, failed to give any signals being received by the probe.

4.2.6 During the calibration of the receivers, it

was also noted that depending on the IF bandwidth, the receiver gave responses at a series of positions of its dial, for every signal of a particular frequency, injected from the signal generator into the receiver. Thus if the discharge emitted simultaneous signals at a number of frequencies, the observed response of the receiver would be expected to be a combination of all the series of responses for each individual frequency.

In order to distinguish between the individual frequencies of oscillations of the discharges, from the total number of responses obtained at the receiver, different signals from the signal generator were injected into the receiver, along with those from the discharge tube. The beat notes obtained at various frequencies were noted, and the value of the individual oscillations of the discharge could then be obtained by refering to the calibration curves of receiver responses against signal generator frequencies.

4.2.7 The output of the receiver could be displayed on a Cossor double beam oscilloscope (Type 1035). At each frequency of oscillations, the received signal appeared to be produced by a series of very narrow pulses at a repetition rate of a few kc/s. The time from the start to the peak of the pulse was about 2.0 microseconds and the total pulse about 40 microseconds. The repetition rate of these pulses was found to vary with the discharge current but, because of their

random distribution over the beam of the oscilloscope, an estimate of the variation could not be made. The total width of the pulse appeared to be unaffected.

The amplitude of these pulses, as seen on the oscilloscope could be calibrated, for different gains of the receiver, from the known level of the input signal generator, by using the thermistor bridge. The level of the intensity of oscillations from the discharge tube was estimated from this calibration of the heights of the pulses as seen on the oscilloscope.

4.2.8 As mentioned earlier, a random electrical 'noise' was always present, along with the oscillations detected at discrete frequencies. This noise was found distributed uniformly over the entire range investigated, except between 450-1000 Mc/s, wherein it was found to reduce gradually to a minimum at about 650 Mc/s and to rise again thereafter. The amplitude of the noise was found to be independent of the tuning of the receiver, as well as the tuning of the Lecher-wire coupling. Any screen cage was not used, since the noise was found to be more characteristic of the discharge than of an external electrostatic origin. Further the discharge tube was required to be kept out of any shielding for irradiation by external visible light. In some cases, simple R-C filters were effective to reduce the spurious circuit oscillations.

4.2.9 By varying the position of the coupling electrodes along the tube, it was found that the maximum intensity could be obtained for the oscillations, as estimated from the calibrated heights of the pulses displayed on the oscilloscope, when the coupling hemi-cylinders were enveloping the cathode dark space. This conformed to the results of Cobine & Gallagher (1947)[a&b] and of Neill & Emeleus (1951). In fact, except for the highest pressures in the case of air and for the two higher pressures in the case of hydrogen, no oscillation could be picked up with the coupling anywhere else on the tube, than around the cathode dark space.

4.2.10 Since a connection between the L/F oscillations and the striations in the positive column is indicated by some workers [Loeb (1947, p. 573), Labrum & Bigg (1952)] , attempt was made to measure the low frequencies of oscillations of the striations. The Cossor oscilloscope, which had an amplifier with a nearly uniform response between about 50 c/s and 1 Mc/s, and which was provided with time and voltage calibrating devices, was found to be a convenient detector for lower frequencies. A photo-multiplier (Type RCA 931), with a fine slit in front, was made to look at the edge of a striation and its output was displayed on the second beam of the oscilloscope. Oscillations, characteristic of the discharge were observed at a frequency of about 200 kc/s. These

were distinct from random noise, and the frequency was dependent on the pressure and the discharge current.

4.2.11 Measurements of the frequencies and the intensities of the H/F oscillations of the discharge were made in the case of both hydrogen and air, with and without external irradiation, while those for the frequencies of oscillations of the striations were only made without irradiation. (Under irradiation the photomultiplier could not detect movements of striations). All these measurements were made along with the probeand discharge current measurements, as described in section I of this chapter, and hence the values of pressures and discharge current were the same as in tables I to VIII of section I. These results are given on the following pages in tables IX to XII in the case of air and tables XIII to XVI in the case of hydrogen. The general trend of results was a diminution in the intensity of the oscillations on exposure to light, as measured from the heights of the pulses, displayed on the oscilloscope. In only a few cases a distinct change in the frequency of the oscillations was observed.

TABLE IX

Measurements of the strengths and the frequencies of the H/F oscillations from a discharge in air at a pressure of p = 1.35 mm. Hg.

Key to the index numbers of the horizontal rows: (1) The freqency of oscillation in Mc/s. (2) The estimated amplitude of the signal as fed to the receiver $\lambda^5 \times 10^{-7}$ watts. This was less by an unknown factor, from the expected amplitude of the generated signal in the discharge (see 4.2.5.). (3) The frequency, at which the striations were seen to be oscilating in the positive column of the discharge by a photomultiplier, in (Kc/s).

Total Discharge Current in Dark.		in Dark	under Light	in Dark	under Light	in Dark	under Light	in Dark	under Light
	(1)	24	24	42	42	169	169	451	451
1.30 mA	(2)	3.2	2.8	6.8	5.9	0.4	0.4	18.3	16.5
	(3)	238							
	(1)	24	24	42	42	131	131	451	451
1.98 mA	(2)	3.1	2.8	6.0	5.2	7.6	6.1	18.0	16.3
	(3)	238							
	(1)	24	24	42	42	131	131	451	451
2.52 mA	(2)	2.9	2.6	5.8	5.1	6.9	5.6	17.8	15.9
	(2)	238.2							
	(1)	24	24	42	42	131	131	451	451
2.95 mA	(2)	2.4	2.0	5.6	4.9	6.9	5.5	17.2	15.1
	(3)	238.2							

TABLE X

Measurements of the strength and the frequencies of the H/F oscillations from a discharge in air at a pressure of p= 1.56 mm.Hg.

For key to the index numbers of the horizontal rows, see Table IX on p.75.

Total Discharge Current in Dark		in Dark	under Light	in Dark	under Light	in Dark	under Light	in Dark	under Light
	(1)	24	24	42	42	169	169	451	451
1.49 mA	(2)	1.9	1.3	5.2	5.0	8.3	7.9	16.8	14.9
	(3)	241							
	(1)	24	24	42	42	169	168	451	451
2.07 mA	(2)	0.8	0.5	4.8	4.1	8.3	7.8	16.3	14.1
	(3)	241							
	(1)	--	--	42	42	169	168	451	451
2.60 mA	(2)	--	--	3.9	3.2	7.8	6.9	15.7	13.2
	(3)	241							
	(1)	--	--	42	42	169	167	451	451
3.16 mA	(2)	--	--	2.8	2.5	6.6	6.0	15.0	12.6
	(3)	241							

TABLE XI

Measurements of the strength and the freqencies of the H/F oscillations from a discharge in air at a pressure of p = 1.86 mm. Hg.

For key to the index numbers of the horizontal rows, see Table IX on p.75.

Total Discharge Current in Dark		in Dark	under Light	in Dark	under Light	in Dark	under Light
	(1)	42	42	169	167	451	451
1.69 mA	(2)	2.1	1.5	6.0	5.7	14.6	12.4
	(3)	241.5					
	(1)	++	--	169	167	451	451
2.22 mA	(2)	--	--	5.3	4.6	13.9	11.9
	(3)	241.5					
	(1)	--	--	169	167	451	451
2.72 mA	(2)	--	--	4.5	3.6	11.9	10.1
	(3)	242					
	(1)	--	--	169	167	451	451
3.21 mA	(2)	--	--	2.9	2.2	10.2	8.8
	(3)	242					

TABLE XII

Measurements of the strength and the frequencies of the H/F oscillations from a discharge in air at a pressure of p = 2.12 mm. Hg.

For key to the index numbers of the horizontal rows, see Table IX on p.75.

Tptal Discharge Current in Dark		in Dark	under Light	in Dark	under Light
	(1)	169	167	451	451
1.90 mA	(2)	1.9	0.5	9.4	8.1
	(3)	244.			
	(1)	--	--	451	451
2.40 mA	(2)	--	--	9.2	7.8
	(3)	244			
	(1)	++	--	451	451
2.89 mA	(2)	--	--	8.3	7.3
	(3)	244.5			
	(1)	31.2	31.0	451	451
3.38 mA	(2)	1.7	0.5	7.7	6.2
	(3)	244.5			

TABLE XIII

Measurements of the strength and the frequencies of the H/F oscillations from adischarge in hydrogen at a pressure p = 1.25 mm. Hg.

Key to the index numbers of the horizontal rows; (1) the frequency of oscillation in Mc/s. (2) The estimated amplitude of the signal, as fed to the receiver X 10^{7} watts. This was less by an unknown factor, from the expected amplitude of the generated signal in the discharge (see 4.2.5). (3) The frequency in Kc/s, at which the striations were seen to be oscillating in the positive column of the discharge, by a photo-multiplier.

Total Discharge Current in Dark.		in Dark	under Light	in Dark	under Light	in Dark	under Light	in Dark	under Light
	(1)	58	57.5	118	118	172	172	362	362
1.55 mA	(2)	18.6	18.1	6.5	6.2	3.9	2.8	21	19.9
	(3)	284							
	(1)	58	57.5	118	118	172	172	362	362
2.27 mA	(2)	18.4	17.9	5.2	4.7	3.2	2.0	18	17.3
	(3)	284							
	(1)	58	57.5	118	118	172	172	362	362
2.95 mA	(2)	18.0	17.4	3.1	2.3	1.9	0.9	17.6	17.0
	(3)	2840							
	(1)	58	58	118	118	--	--	362	362
3.5 mA	(2)	17.6	17.2	2.6	0.9	--	--	17.1	16.5
	(3)	285.5							

TABLE XIV

Measurements of the strength and the frequencies of the H/F oscillations from a discharge in hydrogen at a pressure p = 1.8 mm. Hg.

For a key to the index numbers of the horizontal rows, see Table XIII on p.79.

Total Discharge Current in Dark.		in Dark	under Light	in Dark	under Light	in Dark	under Light
	(1)	58	58	118	118	362	362
2.02	(2)	17.2	16.6	0.5	0.1	16.4	15.7
	(3)	286					
	(1)	58	58	--	--	362	362
2.64 mA	(2)	16.7	16.0	--	--	16.0	14.9
	(3)	286					
	(1)	58	58	--	--	362	362
3.17 mA	(2)	16.1	15.3	--	--	15.3	14.0
	(3)	286					
	(1)	58	58	--	--	362	362
3.80 mA	(2)	15.3	14.7	--	--	14.7	13.3
	(3)	286.5					

TABLE XV

Measurements of the strength and the frequencies of the H/D oscillations from a discharge in hydrigen at a pressure p = 2.5 mm. Hg.

For a key to the index numbers of the horizontal rows, see Table XIII on p.79.

Total Discharge Current in Dark.		in Dark	under Light	in Dark	under Light	in Dark	under Light
	(1)	58	58	--	--	362	362
2.12 mA	(2)	14.6	14.0	--	--	13.9	12.8
	(3)	287					
	(1)	58	58	--	--	362	362
2.71 mA	(2)	13.9	13.1	--	--	13.0	12.1
	(3)	287					
	(1)	58	58	--	--	362	362
3.34 mA	(2)	13.1	12.1	--	--	12.3	11.3
	(3)	287					
	(1)	58	58	210	210	362	362
3.92 mA	(2)	12.4	11.2	1.6	1.6	11.7	10.8
	(3)	287					

TABLE XVI

Measurements of the strength and the frequencies of the H/F oscillations from a discharge in hydrogen at a pressure p = 2.85 mm. Hg.

For a key to the index numbers of the horizontal rows, see Table XIII on p.79.

Total Discharge Current in Dark.		in Dark	under Light	in Dark	under Light	in Dark	under Light
	(1)	58	58	210	210	362	362
2.30 mA	(2)	11.5	10.2	1.4	1.4	11.0	10.1
	(3)	287					
	(1)	58	58	210	210	362	362
2.88 mA	(2)	10.7	9.0	0.9	0.9	10.0	9.4
	(3)	287.5					
	(1)	58	58	--	--	362	362
3.46 mA	(2)	9.6	8.1	--	--	9.0	8.6
	(3)	287.5					
	(1)	58	58	--	--	362	362
4.09 mA	(2)	8.9	7.7	--	--	7.8	7.3
	(3)	287.5					

SECTION III: STUDY OF THE TIME LAG.

4.3.1 Although the reduction of the discharge current on exposure to visible light appears to be instantaneous, a certain time-lag could be conceived for any process or processes responsible for the effect of visible light. An attempt was, therefore, made to obtain some information, if possible, about the processes involved, by studying the time-lag in the reduction of the discharge current, on exposure to visible light.

4.3.2 One of the ways to study the time-lag of the effect was to use a suitable type of shutter mechanism in front of the irradiating source. Since some preliminary experiments designed to measure the time-lag up to 10 μ sec have failed to give any results, it was ~~thus~~ imperative that the shutter mechanism had to operate preferably within a time of 0.1 μ sec. Any mechanical type of high-speed shutter, such as two contra-rotating discs, could give an exposure to better than one μ sec, but had the disadvantage that, when operated in front of a lamp, it could not give pulses of light of enough intensity. A Kerr-cell combination was another possibility but due to the absorption of light in the liquid of the cell, the transmitted light is not intense enough to show any effect.

4.3.3 A Stroboflood† lamp was, therefore, chosen as a

---

†Dawe Instruments (London) Ltd.

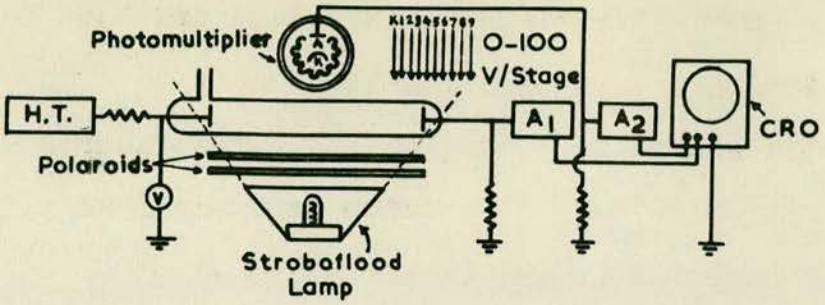

FIG. 13.

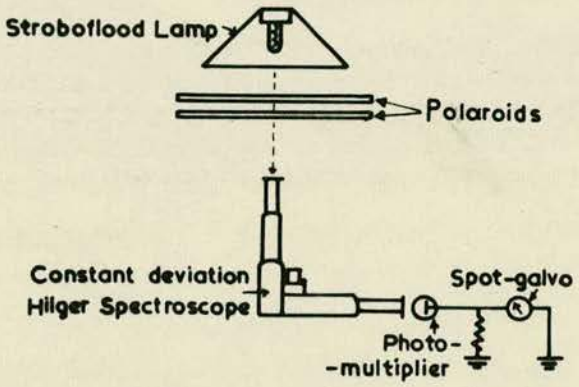

FIG. 15

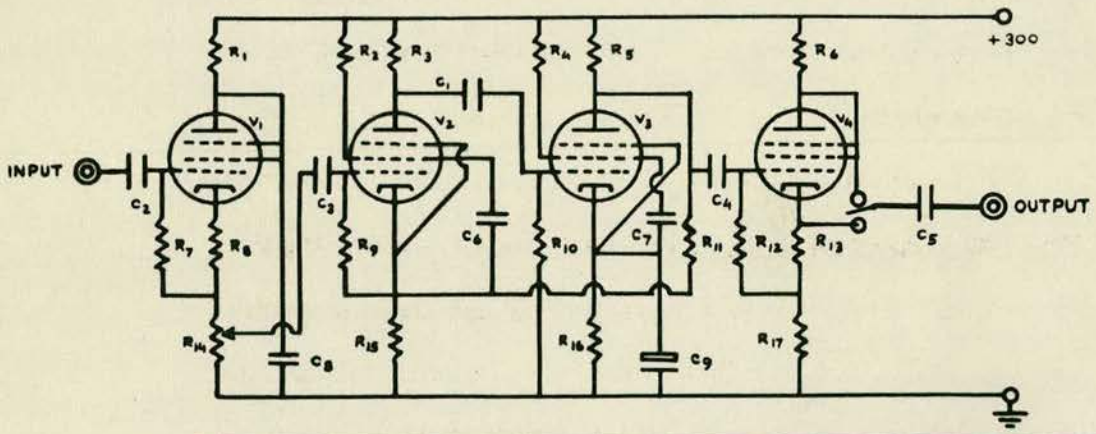

R_1, R_3, R_5 } 4·7k Ω	R_2, R_4, R_6, R_{17} } 22k Ω	R_7, R_9, R_{10}, R_{12} } 1MΩ	R_8, R_{13} } 220Ω; R_{11} } 68kΩ	R_{15}, R_{16} } 1kΩ; R_{14} } 25kΩ POT	C_1, C_2, C_3, C_4 } 0·1μF	C_5 } 0·25μF; C_6, C_7 } 1·0μF	C_8 } 4μF; C_9 } 120μF electrolytic + 0·01μF mica	V_1, V_2, V_3, V_4 } VR 65

FIG. 16.

source to give short intense pulses of light and the frequency of the pulses was controlled by using a standard Stroboflash unit to trigger the Stroboflood lamp. The arrangement was found quite convenient to obtain intense bursts of light (about 1 joule per flash) at a repetition rate that could be varied from 10/sec. to 100/sec. The flash duration was about 20 μsec. at half-peak intensity. The experimental set-up was as shown schematically in Fig. 13. The lamp was kept in front of the discharge tube which was kept in dark. The discharge current was found to diminish on exposure to each irradiating flash and these pulses of the discharge current were observed on a C.R.O. The light pulse was not perfectly square but had its own characteristic curve. Hence the behaviour of this light pulse at various repetition frequencies had to be studied. These light pulses were observed on the second beam of the same C.R.O. by using a photoelectric cell. A RCA 931 photomultiplier was found advantageous since, being a very hard-type cell, it had a good response up to 10^{-7} sec. The cell was independently calibrated by using a rotating disc with a slit in front of a steady lamp. The square pulses of light up to 10 μsec. width were seen to be faithfully recorded by the photomultiplier. In the actual experiments the light of the Stroboflood was too intense for a multiplier and the cell had to be protected by using a very small (pin hole) aperture in

front of the photosensitive cathode. The multiplier was kept in front of the same lamp used to irradiate the discharge tube and its output was fed to the second beam of the C.R,O. (see Fig. 13). These two pulses, one of the discharge current and the other of the irradiating flash were seen simultaneously on the C.R.O. as shown below in Fig. 14.

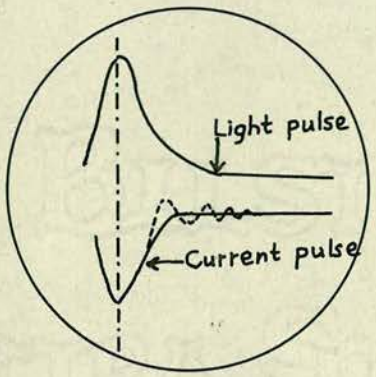

FIG.14

4.3.4 The current pulse, as seen on the C.R.O., often exhibited some ringing towards the trailing end (shown dotted in Fig. 14). This was mainly due to the fact that the two amplifiers operating the two beams of the C.R.O. had different sensitivities and very often the picture was not the same when the two pulses were interchanged on the two beams. The ringing was attributed to some spurious oscillations in one of these amplifiers. Since it was desirable to see exactly how the light and current pulses behave, it was necessary to eliminate this uncertainty of the amplifiers. This was achieved by designing and wiring up two exactly identical amplifiers. The circuit diagram for these D.C. amplifiers is given in Fig. 16.

The total gain was about 50. The output could be obtained as either a positive or a negative pulse by coming out either off the cathode follower or off the anode load. This was useful to reverse the picture of one of the two pulses seen on the C.R.O. for easy comparison. Each amplifier has its own independent gain control. Both these amplifiers were wired-up point-to-point identical at each stage and were tested with a standard square pulse generator. The output pulse was undistorted up to one μ sec. These two amplifiers were then made to replace those on the scope and the output of each was fed directly to the y_1 and y_2 plates. The ringing effect on one of the two pulses disappeared (as expected) with the use of the two new amplifiers. Shielding of the output cables was paid attention to, in order to avoid any stray pick-ups in the circuit.

4.3.5 The behaviour of the light and current pulses was now studied by changing the repetition frequency of the irradiating flashes. The following were the main points observed:

4.3.5(a) LIGHT PULSE: (1) the light pulse did not exhibit a change in its shape. This was consistent with the knowledge that the duration of the flash is characteristic of the power going in to the flash lamp and is independent of the repetition frequency.

(2) The width of the pulse at half-peak

intensity was measured to be 29 μsec. at the repetition frequency of 100/sec.

(3) The amplitude of the light pulse which was proportional to the peak intensity of light emitted by the flash lamp, gradually fell with increase in the repetition frequency, suggesting that the light intensity of the lamp diminished gradually with higher repetition frequencies (see Fig. 19).

4.3.5(b) CURRENT PULSE: (1) The amplitude of the current pulse which was proportional to the effect of external light, first remained unchanged when the repetition frequency was changed from 10/sec. to 50/sec. but later on it dropped by 12% between 50/sec. and 58.3/sec and again remained unaltered up to 100/sec.

(2) This drop in the effect was not observed particularly at any one repetition frequency, but was gradual between 50/sec and 58.3/sec.

4.3.6 Since the behaviour of the light pulse had suggested that there was a change in intensity with frequency, it could bring out a corresponding reduction in the light effect, seen as a reduction in the amplitude of the current pulse. Although this change in the irradiative intensity with the repetition frequency was spread over the entire range of 10/sec. to 100/sec, whereas the change in the amplitude of the current pulse was only observed mainly in the range of 50 to 58.3/sec, it was of much interest to cut down the intensity of light by an amount equal to

the observed reduction associated with a change of frequency from 50 to 58.3/sec and note the corresponding reduction in the current pulse. A simple method of changing the intensity of irradiation was to take the source away from the discharge tube, with the intensity falling according to the inverse square law. However, this had two main disadvantages: (a) as the source was taken away, the discharge tube had to be protected from any stray light, and this problem of moving the source on a light-tight path was tedious to operate experimentally; also (b) the relation between the distance and the intensity being of a square power, the accuracy of moving the source to get very small changes in intensity demanded elaborate modifications. An easier method of controlling the intensity with precision was adapted by introducing two polaroids in between the lamp and the discharge tube. It was then a simple matter of controlling the intensity of light falling on the tube by changing the orientation of the axes of the polaroids. One of them was kept locked and the other rotated relative to the first.

4.3.7 With this arrangement the experiment described earlier in 4.3.5 was repeated. The polaroids were initially kept with their axes parallel to each other allowing maximum transmission. The current pulse did not change in amplitude till 50/sec. As the repetition flash frequency was further increased

from 50/sec to 58.3/sec, the amplitude of the current pulse was reduced by 12%. The amplitude of the light pulse also changed a little as the irradiating intensity dropped down. This new position of the peak of the light pulse was marked on the face of the C.R.O. The flash frequency was then lowered to 50/sec, and both the pulses regained their original amplitudes. Now keeping the flash frequency fixed at 50/sec. the orientation of the polaroids was so changed to bring down the amplitude of the light pulse to its marked value at 58.3/sec. However, the corresponding change observed in the current pulse was only 2.5%. This suggested that the observed reduction in the light effect between flash frequencies of 50/sec and 58.3/sec. was more characteristic of the change in the flash frequency than of the change in the light intensity which was associated with a change in flash frequency.

4.3.8 However, before this change could be attributed to the repetition flash frequency, another interesting point was observed. When the orientation of the polaroids was changed towards cut-off the transmitted light was seen to be more and more purple. It indicated that the problem of controlling the intensity with polaroids was complicated in as much as three parameters were simultaneously involved. First, the flash lamp of the Stroboflood emitted a

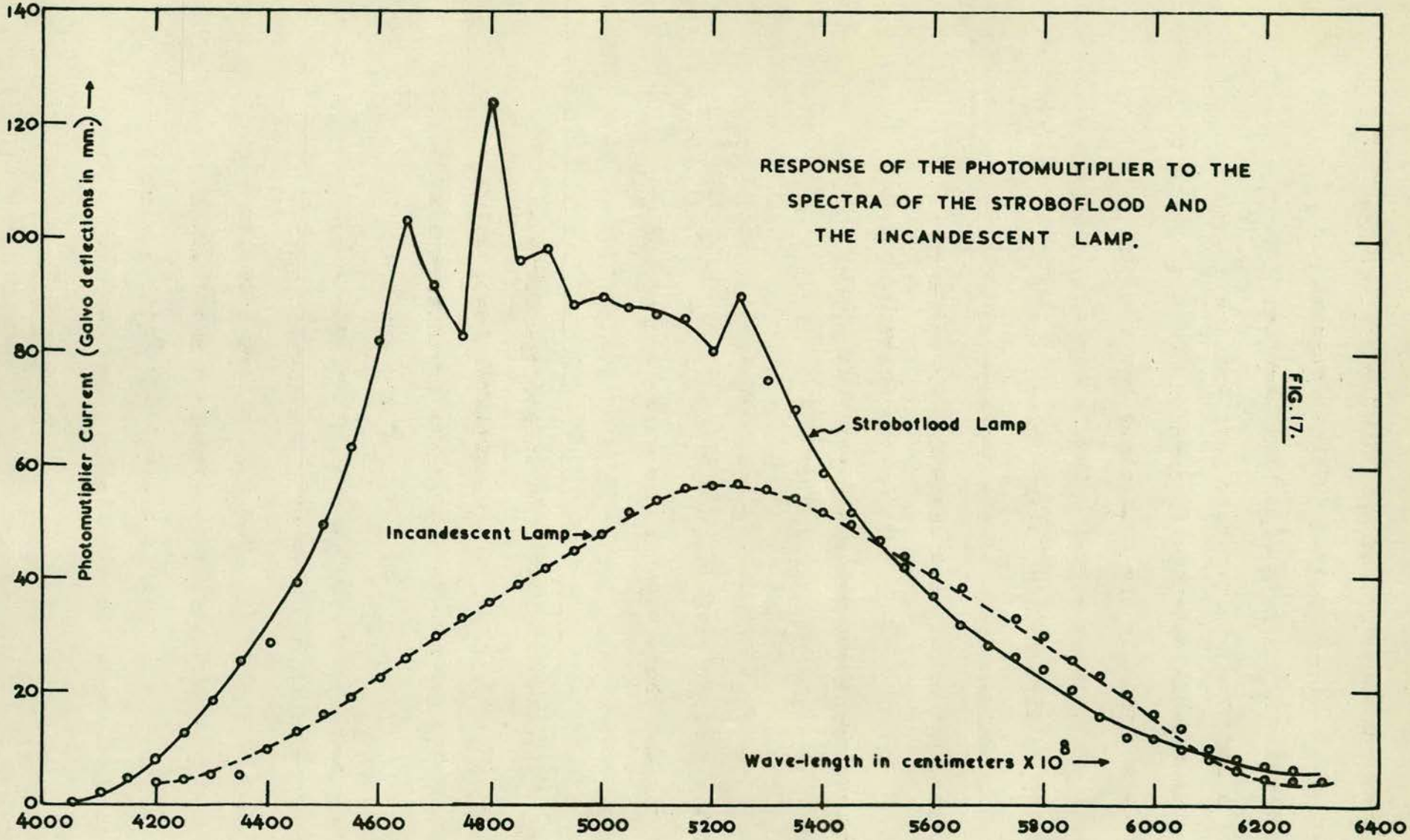
RESPONSE OF THE PHOTOMULTIPLIER TO THE SPECTRA OF THE STROBOFLOOD AND THE INCANDESCENT LAMP.
Photomutiplier Current (Galvo deflections in mm.) →
Stroboflood Lamp
Incandescent Lamp →
Wave-length in centimeters X 10^8 →
0
20
40
60
80
100
120
140
4000
4200
4400
4600
4800
5000
5200
5400
5600
5800
6000
6200
6400

FIG. 17.

line spectrum superimposed on a wide band (roughly between 3500 Å to 6500 Å). With different orientations of the polaroids, this band was cut off to a narrower and narrower part but the transmitted part was also shifting towards one end of the spectrum and finally the multiplier had its own spectral sensitivity curve. The variation in light intensity as effected by polaroids was noted by measuring the amplitude of the light pulse as seen on C.R.O.; but as we were operating in different parts of the spectrum for different orientations of the poloroids, there was every possibility that the amount of variation shown on the C.R.O. may not be the true variation in intensity. To analyse these changes a further calibration of the set up became necessary and these experiments were carried out as follows:

4.3.9 A constant deviation Hilger spectrometer was used to obtain the various spectral sensitivity curves. The general set up of the experiment was as shown in Fig. 15. The drum of the spectrometer was initially calibrated with a Hg-arc spectrum obtained by using the tube of a commercial Hg-arc rectifier as a source. The Stroboflood lamp was then used as a source and its spectrum was studied by the photo-multiplier as a detector. This is shown in Fig. 17 by a continuous line. In the same

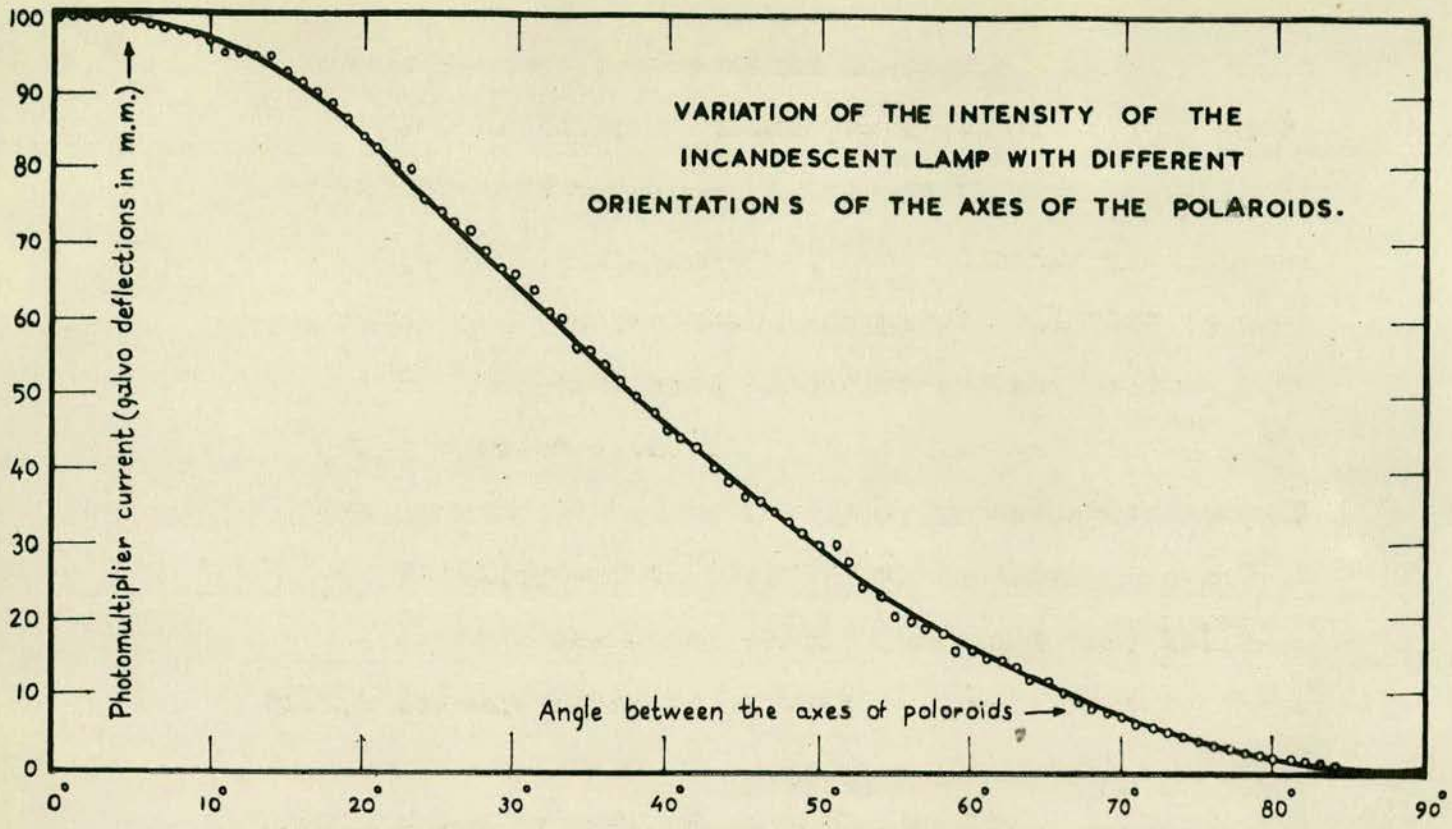
VARIATION OF THE INTENSITY OF THE
INCANDESCENT LAMP WITH DIFFERENT
ORIENTATIONS OF THE AXES OF THE POLAROIDS.
Photomultiplier current (galvo deflections in m.m.) →
Angle between the axes of poloroids →
100
90
80
70
60
50
40
30
20
10
0
0°
10°
20°
30°
40°
50°
60°
70°
80°
90°

FIG. 18.

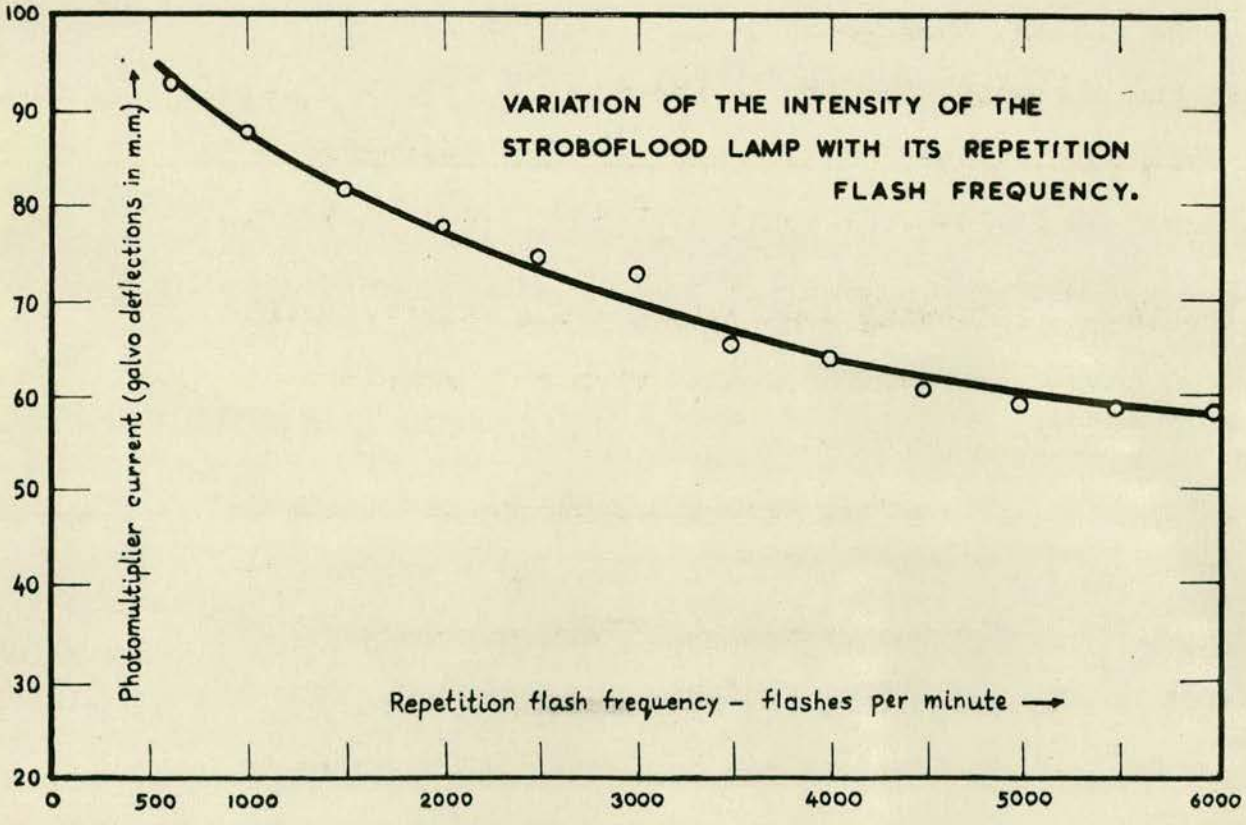
VARIATION OF THE INTENSITY OF THE
STROBOFLOOD LAMP WITH ITS REPETITION
FLASH FREQUENCY.
Photomultiplier current (galvo deflections in m.m.) →
Repetition flash frequency – flashes per minute →
100
90
80
70
60
50
40
30
20
0
500
1000
2000
3000
4000
5000
6000

FIG. 19.

figure the spectrum of an incandescent lamp is also shown (dotted curve) using the multiplier as the detector. This dotted curve, which is the spectral sensitivity curve for the photomultiplier shows a peak at 5250 Å. Using the incandescent lamp again as a source, the two polaroids were inserted between the lamp and the slit of the spectrometer, and the variation of photo-current as a function of the various settings of the axes of the polaroid was studied. (See Fig. 18). This curve was plotted with the drum fixed at 5250 Å, at which the multiplier was found to be most sensitive. The behaviour of the spectral curve of the Stroboflood lamp for various settings of the polaroids was studied next, and the results are given in Fig. 20. From these curves it is evident that there is no selective absorption by the polaroids (as far as the photo-multiplier is concerned), since the reduction of the amplitude of each peak follows the curve of Fig. 18 very closely.

4.3.10 Following conclusions could then be drawn from these calibration figures with reference to the previous experiments.

(1) It was evident that although the transmitted light appeared to be more and more purple to the eye towards increasing difference of angles between the axes of the polaroids, the photomultiplier was immune from this change and hence the light pulse as

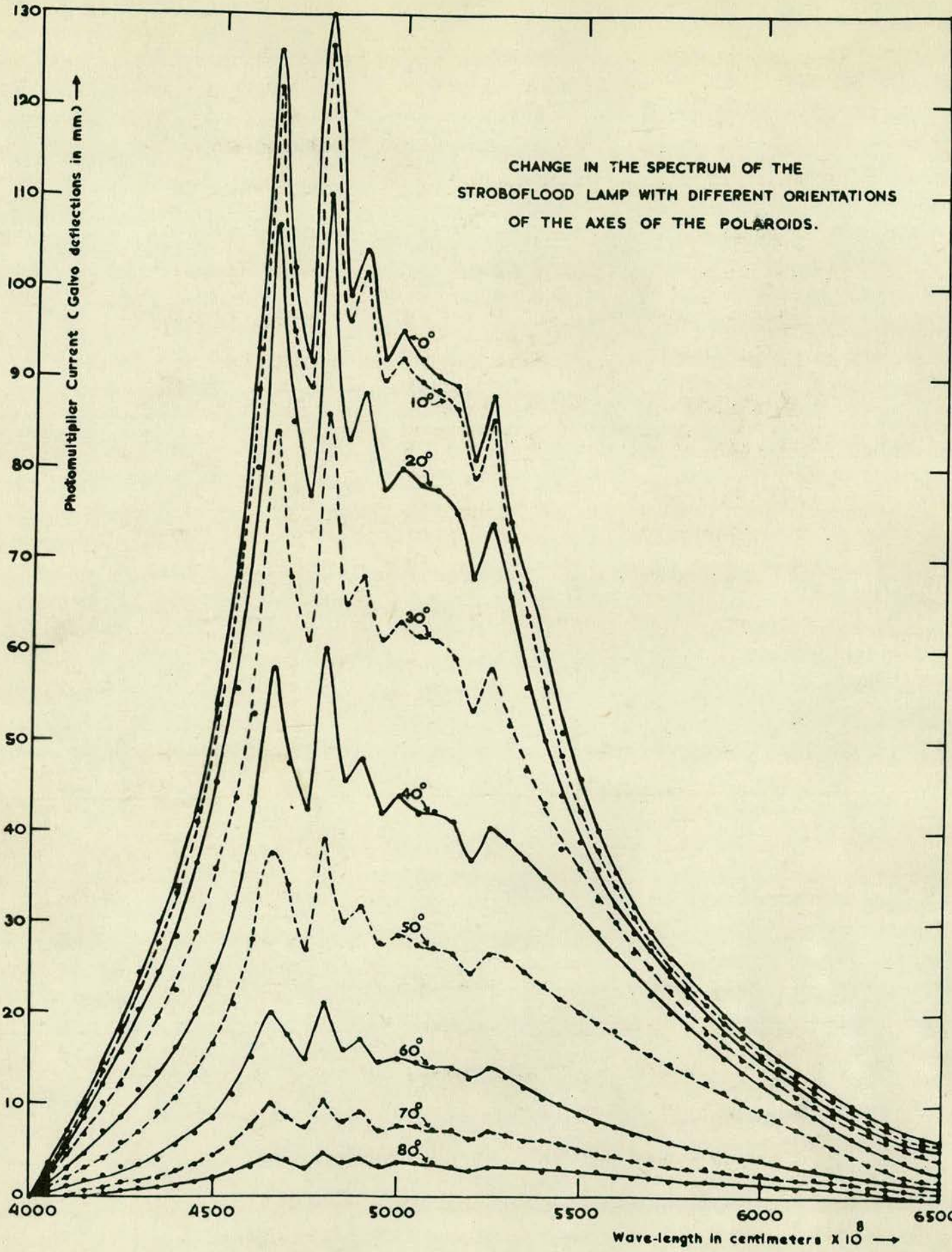
CHANGE IN THE SPECTRUM OF THE
STROBOFLOOD LAMP WITH DIFFERENT ORIENTATIONS
OF THE AXES OF THE POLAROIDS.
Photomultiplier Current (Galvo deflections in mm) →
Wave-length in centimeters X 10⁸ →
0°
10°
20°
30°
40°
50°
60°
70°
80°
0
10
20
30
40
50
60
70
80
90
100
110
120
130
4000
4500
5000
5500
6000
6500

FIG. 20.

seen on C.R.O. was a true representation of the intensity of the transmitted light.

(2) Although the photomultiplier is not much affected by such a change in the colour, this might affect the discharge current, since the light effect is known to vary with the frequency of the irradiating source (vide 1.5.6). But, if the transmitted light is shifting more towards the blue side of the spectrum, the effect should, in fact, increase, causing an increase in the amplitude of the current pulse. This eliminated the possibility that the reduction in the amplitude of the current pulse with increasing angle between the axes of the polaroids was due to the spectral shift of the transmitted light. Therefore, the condition that the light pulse, as seen on C.R.O., diminishing, was believed to be characteristic of a real change in intensity of the irradiating light.

4.3.11 Thus the results indicate that the change in intensity of the irradiating source associated with the change in repetition frequency of flashes from 5^0/sec to 58.3/sec. could not totally account for the observed reduction in the light effect. The above experiments done in air, were also repeated with the same tube now filled with H_2. The observed reduction in effect was 8.2% between the range of frequency of 50/sec to 66.7/sec.; out of this 3% was due to change

in irradiating intensity. [The order of the light effect for various gases is $O_2 < Air < N_2 < H_2$ (see 1.9.4(a))] . The effect of external light is known to increase with V_a, the applied potential and also with p, the pressure of the gas. (See 1.5.1 and 1.5.3). In these experiments, as the pressure and the field were increased, the initial discharge current and so also the effect of light increased, but for comparison of results, when the gain controls on the amplifiers were adjusted to give a constant amplitude for the current pulse, the percentage effect was observed to be the same every time. Another important point observed was that, although a change in amplitude of the current pulse was seen, there was no significant change in the shape of the pulse, which remained almost constant throughout, about 62 μ sec. wide at the base - slightly less than the width of the light pulse. Also the peaks of the two pulses were exactly located at the same instant, (see Fig. 14), indicating that the effect was maximum when the light intensity was also maximum.

CHAPTER V.

CONCLUSIONS.

5.1 Deductions from Probe Measurements, corroborated by the Measurements of the Discharge Current in parts.

5.1.1 This study was the first systematic investigation of the light-effect in d.c. dishharges, where the better knowledge of the processes of d.c. discharges was used with advantage, by making direct measurements with a probe. From fundamental considerations of the composition of the discharge current, as discussed earlier in 1.8, it appeared that the factors likely to be influenced by visible light were n, the number of charged particles and/or k, the mobility. Detailed consideration of these, as included in 1.9, was strongly suggestive of a change in n due to loss of electrons by attachment. The attachment of electrons would then be responsible for a consequent change in the average mobility of the charged particles.

5.1.2 As discussed earlier in 4.1.5, a simple probe could not be used to obtain direct evidence of an increased formation of negative ions. The concentrations of positive ions, calculated from the saturation positive ion current to a negative probe, were found to decrease on exposure to external light.

The different processes responsible for ionization are discussed at length earlier in Chapter II. The most likely process, as given in 2.4, is ionization by electron collision, since the probability of ionization by electron impact has a maximum value greater than the corresponding quantity in excitation. Thus a diminution in the concentration of positive ions was suggestive of a less number of electrons available for formation of positive ions by collision. Considering the different possibilities for loss of electrons, as given in 1.9, the observed reduction in positive ion concentrations was thought to imply the presence of more negative ions under irradiation. This was believed to be corroborated further, by the observed reduction of the discharge current collected by the outer ring, which was mostly due to electrons, as given in 4.1.9.

5.1.3 The relative increase in the positive ion concentrations obtained by the probe, when it was in the glow of a striation, gave evidence that negative ions were grouped in the inter-striation dark spaces. This also conformed with the observations of Agashe (1951) that the light-effect is maximum when the luminous parts of the positive column are irradiated. The curves by Allis et al (1951) for ionization rates per electron across the discharge suggest that the rate is maximum in the luminous part. Plasma resonance can produce these high ionization rates; and since

the excitation at each point is proportional to the ionization at each point, this should also correspond to the light intensity emitted by various portions of the discharge.

5.1.4 The observed dependence of the effect on the discharge current and on the pressure of the gas was compatible with the results, summarised in 1.5.1 and 1.5.3. The total effect in the case of hydrogen was smaller than that in the case of air. A total absence of any influence of "ageing" in the case of hydrogen was believed to indicate the effect of purity of the gas. The importance of impurities on the life of metastable atoms is mentioned in 2.8.2.

5.1.5 As given later in 5.2.3, indications of a negative space charge on the wall of the discharge tube was obtained, which was probably limiting the flow of electrons to a narrow shell between the wall and the axis of the tube. According to the theory advanced by Joshi (1939, 1945 and 1946) the layers on the walls of the vessel emit photo-electrons under the action of light. No evidence of a presence of additional electrons, under irradiation, was obtained in the present study, either by the probe or by the split-electrode.

5.1.6 The view of Prasad (1945) that when radiations fall on the gas, exciting it to higher vibrational and electronic states, the dielectric constant and

hence the dielectric current decreases, was not applicable to the present work in d.c. discharges wherein the current was definitely an ohmic current.

The role of photo excitation and photo-ionization has been considered previously in 2.7. Frank and Grotrian (1921) have pointed out that atoms or molecules in excited states will have properties entirely different from neutral molecules and in some states may well have a strong electron affinity. The influence of external light on the attachment probability may, therefore, be looked upon by way of an intermediate state of photo-excitation. Photo-dissociation of molecules into atoms is also a possibility, as mentioned earlier in 1.9.4(a). Loeb (1952) has suggested that the dissociative capture of electrons, to form negative ions, could explain many results, especially the quenching of Trichel pulses, the decrease of luminosity and the time-lag. This equation gives a time-lag due to ion-formation of the order of 10^{-7} sec. with electron energies of about 3 eV.

5.2 Deductions from the Noise Measurements.

5.2.1 In the present study, the search for oscillations from the discharge was mainly confined to the high frequencies, in order to obtain some information about the concentrations of electrons, in light of the observed reduction in the electronic part of the discharge current, as collected by the outer ring of

the split electrode. No oscillations were detected in the range of plasma-electronic oscillation frequencies, under conditions suitable for observation of the light effect. The observed oscillations were also not related to plasma-ionic oscillations. They were more characteristic of electrical noise confined to discrete frequencies. Their intensities were too high for any connection with thermal origin.

5.2.2 As mentioned earlier in 4.2.5, the influence of light was absent when the probe, which was investigating near the axis of the discharge tube, was used as a coupling. This was suggestive that the observed oscillations had their origin related more to the movements of electrons than to the movements of ions. The intensity of the oscillations was also found to be maximum when the external coupling was around the cathode dark space, where the electrons acquire most of their energies.

5.2.3 When a probe, investigating close to the walls of the tube, was tried for a coupling, it failed to pick up any signals, as it was probably surrounded by a stable negative space charge on the walls. This could prevent the oscillations of electrons from being picked up by the probe. Under irradiation, since a distinct change in frequency was obtained only in a few cases, a definite identity of the oscillations with electrons, believed to be lost under irradiation,

could not be established.

5.2.4 The signals appeared to be produced by very narrow pulses, whose amplitude decreased on exposure to light (see 4.2.7). The nature of these pulses was similar to those observed by Harries & Engel, (1951) in the case of electrodeless a.c. discharges. However, they could not be ascribed, in the present case, to partial discharges of different regions of electrode surfaces.

5.2.5 The oscillations at which the striations were found to be oscillating in the positive column were coherent at a frequency of about 200 kc/s, as reported by Labrum & Bigg (1952). Although they were not dependent on the external circuit they were more characteristic of a type of relaxation oscillations of the whole plasma than of plasma-ionic oscillations.

5.3 Deductions from the Study of the Time-lag.

5.3.1 From the study of the two pulses of current and light as displayed on the scope (see Fig. 14), it was seen that the peak of the current pulse and the peak of the light pulse were occurring at the same instant. The bases of these pulses, whose durations were about 69 μsec, as mentioned earlier in 4.3.11, were displayed on the scope over a length of about 60 mm. By inverting one of these pulses, with the provision on the amplifier as mentioned in 4.3.4, the

peaks of the two pulses could be compared within at least a millimeter; so the absence of any difference between the peaks of the two pulses up to a millimeter could be regarded as indicating no time lag, between the exposure of the discharge to irradiation and consequent reduction of current, up to 0.8 μ sec. This compares with the figure by Loeb (1952) of 10^{-7} sec. for the time-lag due to ion formation (see 5.1.6).

5.3.2 In the case of air there was no change in the amount of light-effect up to a flash frequency of 50/sec, which would mean that the whole process responsible for the light effect was complete within 20 milliseconds, after which interval the next light pulse occurred. The observed change in the light effect, when the flash frequency was changed from 50/sec to 58.3/sec., was a diminution of 12.0%, out of which 2.5% could be attributed to a change in the intensity of the light pulse, if a linear relation between light intensity and light effect is assumed. Thus, a critical part of the process, which was responsible for 9.5% of the total effect of light, appeared to occur after about 17 milliseconds. When the flash frequency was changed from 58.3/sec. to 100/sec., no further change was observed. This signified that the remaining part of the process was probably occurring before 20 milliseconds and after 17 milliseconds. Whether it did really occur within

3 milliseconds, could not be verified because the maximum of the repetition flash frequency of the triggering Stroboflash unit was unfortunately only 100/sec.

In the case of Hydrogen the corresponding figures were - total process occurring within 20 milliseconds, a critical part, responsible for 5.2% of the total effect occurred after about 15 milliseconds.

5.3.3 The elaborate calibrations performed to study the influences of different parameters involved in the observation, clearly indicated that the observed changes were truly characteristic of the variations in the flash frequency. If the attachment of electrons to form negative ions is regarded as the likely process, responsible for the action of external light, it may be deduced that most of the attachment was taking place within 3 milliseconds in the case of air and within 5 milliseconds in the case of hydrogen, assuming that the remaining major part of the process did complete itself within 3 and 5 milliseconds respectively. Further, in the case of air, the percentage of the total process occurring within this interval of 3 milliseconds (90.5%) was less than that in the case of hydrogen (94.8%) occurring within 5 milliseconds. Thus, statistically over a certain interval of time, the effect of light

in the case of air could be expected more than in the case of hydrogen. This is compatible with the previous results, obtained with a.c. discharges [(see 1.9.4(a)] , that under identical conditions, the effect of external light is more in the case of air than in the case of hydrogen.

ACKNOWLEDGEMENTS.

This study was carried out in the Electronics Section of the Department of Engineering of Edinburgh University, and the author is indebted to Professor R. N. Arnold for the provision of all the necessary research facilities.

Grateful thanks are due to Mr. W. E. J. Farvis, Senior Lecturer in Applied Electricity at the University of Edinburgh, under whose direction the work was undertaken. His helpful counsel and invaluable discussions on many aspects of the experiments are deeply appreciated.

The technical assistance of Mr. T. S. Broom of the Chemistry Department and of Mr. B. Tulloch of the Engineering Department in assembling the glass vacuum systems is also gratefully acknowledged. A part of the vacuum system B, shown in Fig. 6, was originally designed by Dr. S. Kaufman for his experiments and was later adapted for this work.

The research was supported by an award of an Edinburgh University post-graduate studentship, for which the author is indebted to the University.

BIBLIOGRAPHY

A Agashe, V.V. (1951), J.Chem.Phys., 19, 1002.
(1952), Proc.Phys.Soc.(London),B, 65, 740.
Allis, Brown, & Everhart. (1951), Phys.Rev., 84, 519.
Appleton,E.V. & West, A.G.D. (1923), Phil.Mag., 45, 879.
Armstrong, E.B., Emeleus, K.G. & Neill, T.R. (1951),
Proc.R.Irish Acad,A, 54, 291.

B Bloch, F.& Bradbury, N.E. (1935), Phys.Rev., 48, 689.
Boyd, R.L.F. (1950a), Proc.Roy.Soc,A, 201, 329.
(1950b), Nature (London), 165, 142.
Boyd, R.L.F. & Twiddy, N.D. (1954), Nature (London), 173, 633.
Branscomb, L.M. & Fite, W.L. (1954), Phys.Rev., 93, 651.

C Canac, A., Maret, G. & Goldzahl L. (1950),
C.R.Acad.Sci.(Paris), 231, 1054.
Chattock, A.P. (1899), Phil.Mag., 48, 401.
Chattock, A.P. & Tyndall, A.M., (1909), Phil.Mag., 19, 543.
Cobine, J.D. & Gallagher, C.J. (1947a),
J.Appl.Phys., 18, 410.
(1947b), J.Franklin Inst., 243, 41.
Compton, K.T., Turner, L.A. & McCurdy, W.H. (1924),
Phys.Rev., 24, 597.
Coolidge. (1944), Phys.Rev., 65, 236.

D Deo, P.G. (1944), Indian J.Phys., 18, 84.
Deshmukh, G.S. (1947), J.Indian Chem.Soc., 24, 211.
(1949a), Proc.Indian Acad.Sci,A, 29, 243.
Deshmukh, G.S. & Dhar, V.S. (1949b),
J.Indian Chem.Soc., 26, 179.
Donahue & Dicke. (1951), Phys.Rev., 81, 248.

E Eckhart, C. & Compton, K.T. (1924), Phys.Rev., 24, 97.

F Fowler, R.G. (1951), Phys.Rev., 84, 145.
Frank, & Grotrian. (1921), Z.Phys., 4, 89.

G Gale. (1953), Amer.J.Phys., 21, 389.
Gambling, W.A. (1952), Phys.Rev., 85, 677.
Guthrie, A. & Wakerling, R.K. (1947),
The Characteristics of Electrical Discharges in Magnetic Fields, 1st Edition, (New York, McGraw-Hill Book Co., Inc.)

H Harris, W.L. & Von Engel, A. (1951),
Proc.Phys.Soc.(London),B, 64, 916.
Hudson, A.L., Loria, A. & Ryder, N.V. (1930),
Phil.Mag., 41, 828.

J Joshi, S. S. (1939), Current Sci,(India), 8, 548.
Joshi, S. S. & Narsimhrao, V. (1940), Current Sci,(India), 9, 536.
Joshi, S. S. & Deshmukh, G.S. (1941), Nature (London), 147, 806.
Joshi, S. S. & Deo P.G. (1943), Nature (London), 151, 561.
Joshi, S. S. & Deo P.G. (1944a), Nature (London), 153, 434.
Joshi, S. S. (1944b), Nature (london), 154, 147.
(1945), Proc.Indian Acad.Sci,A, 14, 317.
(1946), Current Sci,(India), 15, 281.
Kaufman,S.(1954), Ph.D. Thesis, Edin. Univ.
K Kniepkamp, H. (1936), Zeits.f.Tech.Phys., 17, 397.

L Labrum, N.R. & Bigg, E.K. (1952), Proc.Phys.Soc.(london),B, 65, 356.
Langmuir, I. & Mott-Smith. (1923), Gen.Elec.Rev., 26, 731.
Langmuir, I. (1925), Phys.Rev., 26, 585.
Lau, & Reichenheim. (1929), Ann.Phys., 3, 840.
(1930), Ann.Phys., 5, 296.
Little, P.F. (1953), Abstract - Conference on Ionization Phenomena in Discharges, Oxford.
Loeb, L.B. (1947), Fundamental Processes of Electrical Discharges in Gases, 2nd Edition, (New York, John Wiley & Sons, Inc.)
(1952), Phys.Rev., 86, 256.

M Mallikarjunappa. (1948), J.Indian Chem.Soc., 25, 197.
Massey, H.S.W. & Smith, R.A. (1936), Proc.Roy.Soc,A, 155, 472.
Massey, H.S.W. (1950), Negative Ions, 2nd Edition, (Cambridge, Cambridge University Press.)
Meek, J.M. & Craggs J.D. (1953), Electrical Breakdown in Gases, (Oxford, Oxford Univ.Press.)
Meissner, K.W. & Miller, W.F. (1952), Phys.Rev., 85, 706.
Mohanty, S.R. & Kamath, G.S. (1948a) J.Indian Chem.Soc,, 25, 405.
(1948b), J.Indian Chem.Soc., 25, 466.
Mohanty, S.R. (1949a), J.Indian Chem.Soc., 26, 507.
(1949b), J.Indian Chem.Soc., 26, 553.
(1951), J.Indian Chem.Soc., 28, 487.

N Neil, T.R. & Emeleus, K.G. (1951), Proc.R.Irish.Acad,A, 53, 197.
Newman, E.H. (1924), Phil.Mag., 47, 839.

P Pardue, L.A. & Webb, J.S. (1928), Phys.Rev., 32, 946.
Partridge, J.G. (1949), Glass-to-metal Seals. (Sheffield, Soc.of Glass Tech.)
Penning, F.M. (1928), Physica (Old Series), 8, 137.
(1932), Physica (Old Series), 12, 65.
(1938), Physica, 5, 286.
Prasad R. (1945), Nature (London), 155, 362.
Prasad, B.N. & Jain, T.C. (1947), Proc.Indian Acad.Sci,A, 25, 515.

R Rao, D.V.R. & Sharma, B.K. (1949), J.Phys.& Colloid.Chem., 53, 753.

S Smyth, H.D. (1931), Rev.Mod.Phys., 3, 347.

T Thomson, J.J. (1916), Phil.Mag., 30, 321.
(1928), Proc.Phys.Soc.(London), 11, 79.
Thomson, J.J. & Thomson, G.P. (1933), Conduction of Electricity through Gases, Vol. II, 3rd Edition, (Cambridge, Cambridge University Press.)
Tonks, L. & Langmuir, I. (1929a) Phys.Rev., 33, 195.
(1929b) Phys.Rev., 34, 876.
Townsend, J.S. & Tizard, H.T. (1913), Proc.Roy.Soc,A, 86, 336.
Townsend, J.S. & Bailey, V.A. (1921), Phil.Mag., 42, 873.

V Vishwanathan, K.S. (1949), J.Indian Chem.Soc., 26, 190.

W Wahlin, H.B. (1922), Phys.Rev., 19, 173.

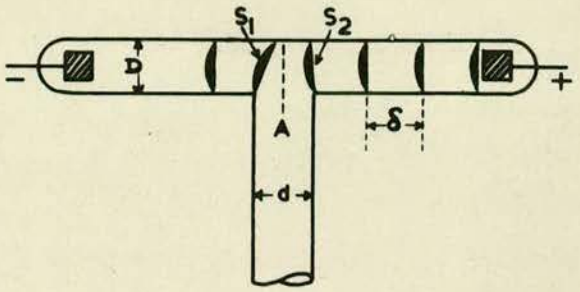

FIG. 21.

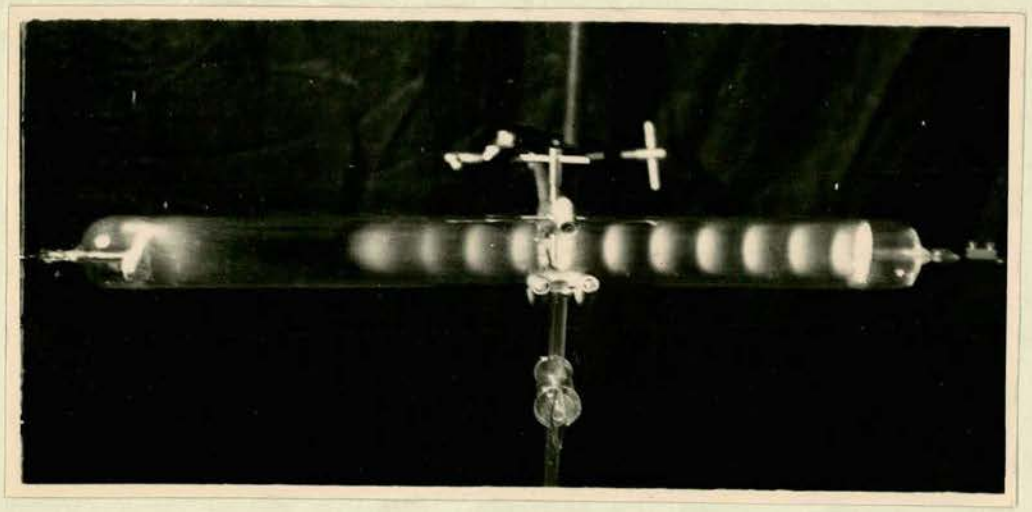

D = 40.05 mm
d = 9.36 mm

Tube A
D/d = 4.275

FIG. 22.

APPENDIX A.

A Note on the Conditions for Formation of Striations in Hydrogen Glow Discharges.

During the investigations about the role of striations in the mechanism of the effect of external light on glow discharges, as discussed in detail earlier in (4·1·7·), another peculiar phenomena about striations was observed, which was later investigated in more detail.

A few months before these observations were made, Fowler (1951) had published a note about a remarkable property of the striations which he observed. In this communication, he has said that no striations ever existed at the Junction A of the side-tube and the main discharge tube (see fig. 21), although stable striations could exist on both sides of A. When the vicissitudes of increasing current compelled striation S_1 to move across the junction, it moved abruptly, and very quickly to the position S_2. In all other positions the striations moved slowly and smoothly along the tube.

The phenomena noted during the course of present research was similar in nature to Fowler's observation. A large discharge tube, 40 mm. in diameter and 440 mm in length, filled with hydrogen at a pressure of 1.2 mm. of mercury, with two internal electrodes was excited with a steady potential difference and it never

showed any striation being formed at the junction when the tube was quite clean. However, this tube once got heated so much during a long experiment, that some grease from a stopcock which was directly below the junction, evaporated. The discharge tube was held in a clamp, which rested exactly over the junction (as seen in the photograph in Fig.22) and the evaporated grease vapour condensed on the relatively cold part of the tube in contact with the clamp. Thus a narrow ring of grease coating was formed on the tube directly above the junction. This made a remarkable change as regards formation of striations; a striation was now found even at the junction (Fig.22) and in fact the whole column of striations could be moved all along the tube slowly and smoothly without any abruptness, which was observed earlier and which is described by Fowler.

Looking at the tube B in Fig.23 , which being clean, confirms Fowler's observation that a striation does not appear across the junction and if we have to account for its absence by a discontinuity in the glass periphery, as suggested by him, it appears that what the glass periphery does for formation of a striation can be compensated by the presence of impurity on the wall of the tube in Fig. 22. The action of such impurity in removal of metastable atoms is well known [Compton et al (1924)]; and the role played by the glasswall can be probably looked

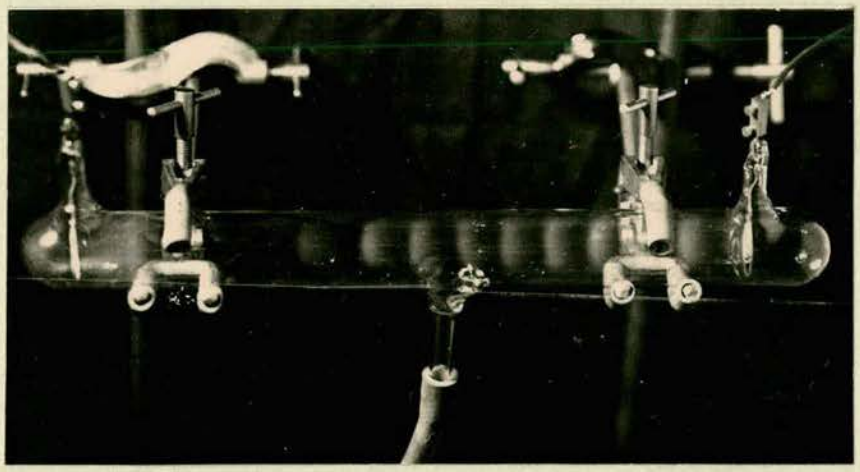

D = 30·75mm Tube B
d = 10·0mm D/d = 3·075

FIG. 23.

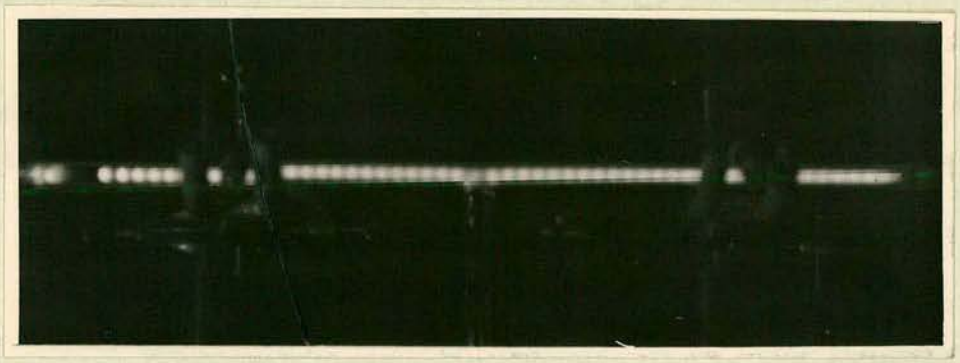

D=9·48 mm Tube C
d=10·0 mm D/d= 0.948

FIG. 24.

upon in this light. We would, therefore, expect Fowler's observed effect to be even more pronounced if we work with a clean tube, which has a wider side-arm causing a wide break in the glass periphery at the junction.

To study this aspect we took a third tube (C) of a smaller diameter but with a side-arm larger in diameter than the main discharge tube (Fig.24). The vacuum system was now provided with a needle valve and both the pressure as well as the applied field could be varied continuously. With this arrangement it was possible to get the striations such that average distance δ (see Fig.21) between two of them was smaller than d, the diameter of the junction opening. When a column of such striations was made to move over the junction, it was curiously observed that a striation could now be seen at the junction, although the tube was clean. (Fig.24). Thus in both clean tubes A and B, when D was greater than d (or when D/d was greater than unity), striations seemed in general, to avoid the junction (Fig.23); but in the case of tube C, where D was less than d (or where D/d was less than unity), they preferred to form across the junction - sometimes with a slight hesitation - than to show any asymmetry in their spacing.

Since a satisfactory theory of striations has not yet been put forward, a complete interpretation of

every striation phenomena is not easy. Lau & Reichenheim (1929 and 1930) have concluded that the recombination of H atoms to H_2 molecules at the wall is important for the appearance of striations. Donahue & Dicke (1951) have concluded as a result of their experiments that the travelling regions of positive and negative space charges, responsible for striations are initiated by the accumulation of electrons in the negative glow region. On the other hand, Loeb (1947 p. 573) has suggested that the striations may be associated with plasma-oscillations. These results are in support of the view of the mechanism of the striations, that they have their origin in the plasma itself. Any electrical wave of sufficiently short length, if propogated through the plasma, would suffer a phase change on reflection at the head of the column and would set up a standing wave. The striations may then be accounted for by the positions of the nodes and antinodes. Recent observations of Gale (1953) with H/F discharges excited by placing the discharge tube between the wires of a Lecher system, show the presence of striations at the voltage antinodes indeed. There are, however, other theories also, advocating the presence of striations as due to the cathode phenomena. Most recent observations of Boyd & Twiddy (1954) giving some preliminary results

about the electron energy distribution in the striated hydrogen discharge, indicate that in a striation, there is present a group of electrons having energies considerably higher than the mean.

Gambling (1952) in commenting on Fowler's observation, has suggested that the increase in the effective diameter at the junction may violate the Druyvesteyn and Penning's (1940, Fig. 78) empirical relation $pR = m$, where p is the pressure of the gas in mm.Hg; R is the radius in cm. and m is a constant depending on the current. However, this does not seem to account fully for the phenomena observed in the present investigation, since there can always be found a condition to satisfy this relation even at the junction, by varying either the pressure or the applied field. Although the pressure and the field were independently changed over a large range in the present investigation, a striation could never be seen across the junction in both tubes A and B, when they were clean and where D/d was greater than unity.

APPENDIX B

A New Device for Breaking the Capillary-Seals of Gas-Bottles.

During the course of this research, a new kind of device was developed and successfully operated for breaking the seals of the gas-bottles. The gas-bottles in which various pure gases are commercially supplied by firms like the British Oxygen Co., are usually supplied in soft soda-glass vessels. However, in high vacuum systems, such as the one used in present experiments, the assembly has often to be made in a hard glass, like pyrex, in order to be able to bake the system for thorough out-gasing. For use on such systems, to facilitate the joining of the gas-bottle directly to the vacuum system without any graded seals, the gases could be specially obtained in pyrex vessels.

The usual method of breaking the capillary seals on these gas bottles is to place a small iron ball inside the vertical neck of the gas-bottle before it is joined to the vacuum system. After evacuation of the neck, the iron ball is lifted by a magnet from outside of the glass neck and is then allowed to drop on the fine capillary seal. This breaks the capillary and allows the gas in the bottle to come out into the neck and then into the system as required.

Although this technique is quite successful for

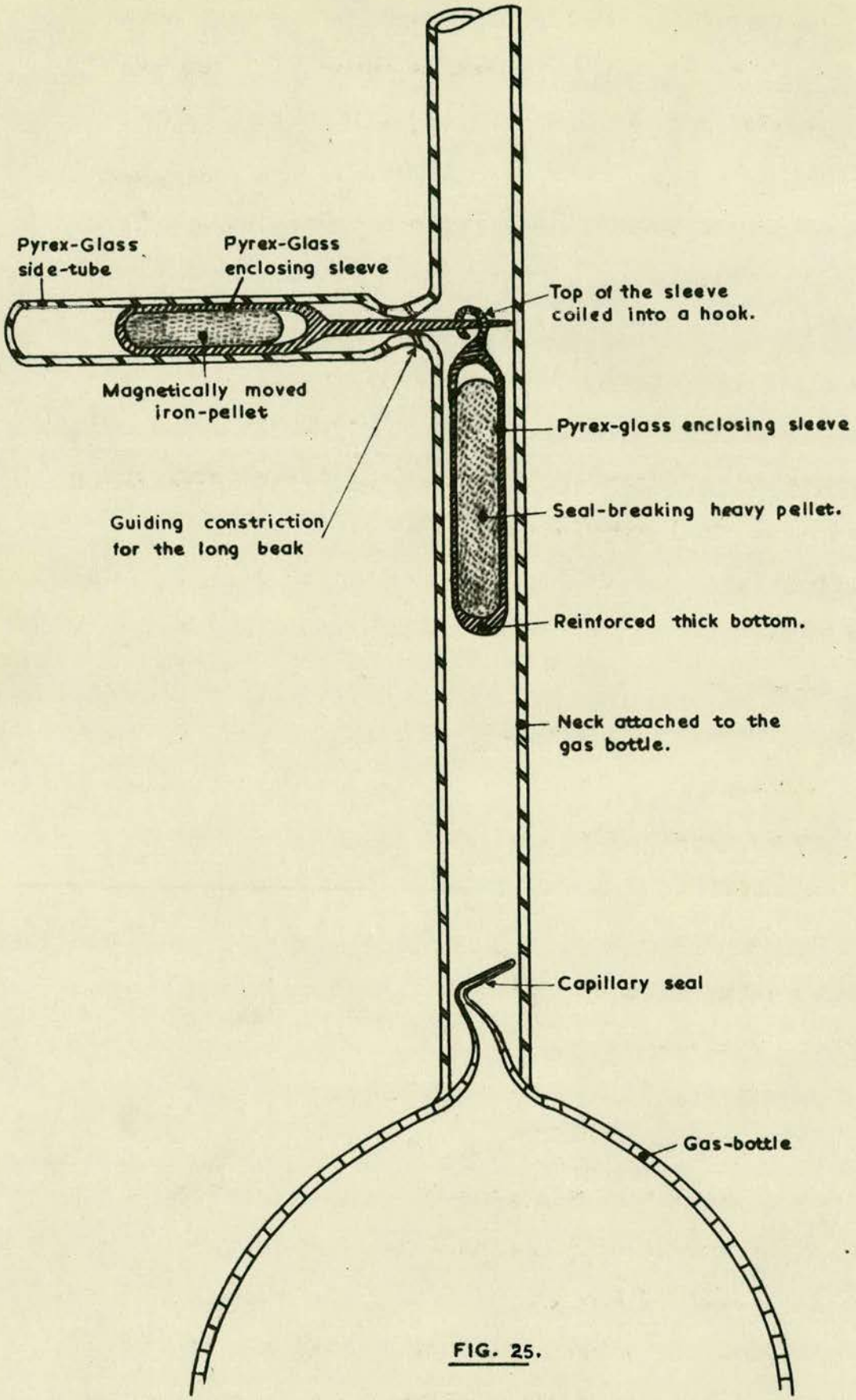
Pyrex-Glass side-tube
Pyrex-Glass enclosing sleeve
Top of the sleeve coiled into a hook.
Magnetically moved iron-pellet
Pyrex-glass enclosing sleeve
Guiding constriction for the long beak
Seal-breaking heavy pellet.
Reinforced thick bottom.
Neck attached to the gas bottle.
Capillary seal
Gas-bottle

FIG. 25.

soft-glass seals, it has often been found that when handling gas-bottles of pyrex, a round ball (as big in diameter as the neck could take) is not sufficiently heavy to break the hard glass capillary and larger cylindrical pellets had to be used. To lift these, a more powerful magnet is required. Further, when the purity of the gas is important, the metal pellet is desired to be totally enclosed in a glass sleeve in order to prevent it from contaminating the gas by out-gassing. With such an enclosing glass sleeve, a still more powerful magnet is required to raise such a heavy cylindrical pellet from outside the two glass walls (one of the enclosing sleeve and the other of the neck). When working in restricted space, with systems compactly set up on small trolleys, the lifting of such heavy pellets by a large magnet is indeed often cumbrous.

To overcome these difficulties, a new arrangement was constructed as shown schematically in detail in the opposite figure. The seal-breaking heavy pellet is suspended in the main neck of the gas-bottle a short distance over the capillary seal, by a glass hook, through which the long beak of the enclosing sleeve of another small pellet is passed. This second pellet is placed in a side-tube, joined to the main neck of the gas-bottle. The free end of the side-tube is initially open and a small constriction is made at its joint with the neck, in order to guide

the long glass beak along a particular direction.

In practice, the system is assembled as follows: a small dimple is first made in the neck of the gas-bottle (not shown in the sketch) above the capillary seal, beyond which the heavy pellet cannot go and break the seal accidently. Then holding the gas-bottle with its neck horizontal and the side-tube vertical, the heavy seal-breaking pellet, which is totally enclosed in a glass sleeve and having a small glass hook on top (see fig.) is slid down the neck till the glass hook is directly below the constriction in the joint of the side tube. The second pellet, which is also enclosed totally in glass and which has a long glass beak, is then put in the side-tube through its open free end, so that its beak passes through the constriction and through the eye of the glass hook below it, till the tip of its beak touches the wall of the neck of the gas-bottle. Some cotton-wool is then packed over it, in the side-tube to prevent it from sliding back. When the gas-bottle is now made to stand with its neck vertical, the heavy pellet is suspended on the beak of the second side-pellet, above the capillary seal.

The gas-bottle is then joined to the vacuum system in this position. When it is secured in its place, the protecting dimple in the neck of the gas bottle is removed by playing a torch over it

and at the same time, blowing through the open end of the side-tube. The packing cotton-wool is then gently removed and the side tube is drawn close, leaving a space roughly equal to the diameter of the neck, behind the side-pellet inside it.

The side-tube and the neck can then be evacuated to the reqqired degree of vacuum and baked out if necessary. In order to break the sealing capillary, the pellet in the side-tube is drawn back, by an outside magnet, towards the dead end of the side tube. This disengages the hook from the beak, releasing the suspended pellet to drop on the capillary seal and break it. The bottom end of the glass sleeve enclosing the dropping pellet is thickened to withstand the impact.

The system has the following advantages:

(1) The pellet in the side-tube can be small, making it possible for a tiny magnet to operate it.

(2) Because of a side-ways motion in the side-tube, the magnetic force required to move the side-pellet is only to overcome the frictional resistance, whereas if a magnet is to lift the striking pellet, the required force is to counteract its gravity. With this device, it has been found that a tiny U-magnet can easily drop a heavy striking pellet.

(3) The required force for breaking the seal of any hard glass can be easily obtained either by choosing a heavier striking pellet or allowing it to

drop from a greater height. Both these factors are independent of the size of the magnet required.

From the little experience obtained so far with this technique, it is observed that the troubles of a little extra glass-blowing, required in making and setting up the device, are amply rewarded by the ease of operation and positive action.

APPENDIX C

Critical Potentials of Hydrogen and other Impurities.

Atom or Molecule	First excitation potential (eV).	Ionization potential (eV)	
		I	II
H	10.2	13.6	--
H_2	11.2	15.6	--
N	6.3	14.5	29.6
N_2	6.1	15.5	--
CO	6.0	14.1	--
CO_2	10.0	13.7	--
O	9.1	13.6	35.2
O_2	--	12.2	--
H_2O	7.6	12.6	--

Landolt - Börnstein: vol. I, (Part I), 1950. Cited by Meek & Craggs (1953).

Cross-section for Excitation (Q_{ex}) of Various Transitions in Atomic Hydrogen. $(cm)^2$

Electron Energy	Elastic Scattering	TRANSITIONS												
		$1_s \rightarrow 2_s$	$1_s \rightarrow 2_p$	$1_s \rightarrow 3_s$	$1_s \rightarrow 3_p$	$1_s \rightarrow 3_d$	$1_s \rightarrow 4_s$	$1_s \rightarrow 4_p$	$1_s \rightarrow 4_d$	$1_s \rightarrow 4_f$	$2_p \rightarrow 3_s$	$2_p \rightarrow 3_p$	$2_p \rightarrow 3_d$	Ionization
eV	$Q_e \times 10^{-18}$	$Q_e \times 10^{-19}$	$Q_e \times 10^{-17}$	$Q_e \times 10^{-19}$	$Q_e \times 10^{-18}$	$Q_e \times 10^{-20}$	$Q_e \times 10^{-19}$	$Q_e \times 10^{-18}$	$Q_e \times 10^{-20}$	$Q_e \times 10^{-22}$	$Q_e \times 10^{-17}$	$Q_e \times 10^{-17}$	$Q_e \times 10^{-16}$	$Q_i \times 10^{-18}$
20	114.4	193.6	14.46	33.46	25.97	54.59	12.32	9.421	30.82	45.69	17.38	15.50	31.38	72.2
50	47.5	95.3	9.98	18.49	17.17	32.58	6.61	6.163	12.32	27.83	10.13	6.34	17.10	122.4
100	26.2	50.2	6.72	9.69	11.44	17.61	3.52	4.051	6.52	10.30	6.34	3.17	10.10	93.3
150	17.8	34.3	5.13	6.61	8.10	11.44	2.47	3.082	4.75	7.48	—	—	—	72.2
200	13.5	25.5	4.16	5.02	7.13	9.69	2.20	2.474	3.70	5.72	—	—	—	59.8
300	9.1	17.6	3.17	—	—	—	—	—	—	—	—	—	—	38.8
400	6.8	13.2	2.55	—	—	—	—	—	—	—	—	—	—	—
700	4.0	7.0	1.76	—	—	—	—	—	—	—	—	—	—	—
1,000	2.7	4.4	1.23	—	—	—	—	—	—	—	—	—	—	—

APPENDIX D.